Phosphate starvation response precedes abscisic acid response in response to mild drought in plants

Yukari Nagatoshi[1], Kenta Ikazaki[2], Nobuyuki Mizuno[3†], Yasufumi Kobayashi[1], Kenichiro Fujii[1], Eri Ogiso-Tanaka[4‡], Masao Ishimoto[4], Yasuo Yasui[3], Tetsuji Oya[2], Yasunari Fujita[1,5*]

[1] Biological Resources and Post-harvest Division, Japan International Research Center for Agricultural Sciences (JIRCAS); Tsukuba, Ibaraki 305-8686, Japan.
[2] Crop, Livestock and Environment Division, Japan International Research Center for Agricultural Sciences (JIRCAS); Tsukuba, Ibaraki 305-8686, Japan.
[3] Graduate School of Agriculture, Kyoto University; Kyoto, Kyoto 606-8502, Japan.
[4] Institute of Crop Science, National Agriculture and Food Research Organization (NARO); Tsukuba, Ibaraki 305-8518, Japan.
[5] Graduate School of Life Environmental Science, University of Tsukuba; Tsukuba, Ibaraki 305-8572, Japan.
[†]Present address: Institute of Crop Science, NARO; Tsukuba, Ibaraki 305-8518, Japan.
[‡]Present address: Center for Molecular Biodiversity Research, National Museum of Nature and Science; Tsukuba, Ibaraki 305-0005, Japan.

Yasunari Fujita[1,5*]
Biological Resources and Post-harvest Division, JIRCAS; 1-1 Ohwashi, Tsukuba, Ibaraki 305-8686, Japan.
[*]Corresponding author. E-mail: yasuf@affrc.go.jp

Author Contributions: Y.N. and Y.F. conceived and designed the study and wrote the paper; Y.N. performed most of the experiments and analyzed the data; K.I. performed the soil and chemical analyses; Y.N., K.F., and Y.F. performed the field experiments, with support from T.O. and Y.K.; Y.N., N.M., Y.K., E.O-T., M.I., and Y.Y. performed the transcriptome analysis. All authors discussed and commented on the manuscript.

Competing Interest Statement: The authors declare no competing interests.
Classification: Biological Sciences, Plant Biology.

Abstract

Drought severely damages crop production, even under conditions so mild that the leaves show no signs of wilting. However, it is unclear how field-grown plants respond to mild drought. Here, we show through 6 years of field trials that ridges are a useful experimental tool to mimic mild drought stress in the field. Mild drought reduces inorganic phosphate levels in the leaves to activate the phosphate starvation response in soybean plants in the field. Using the model plant *Arabidopsis thaliana* grown in pots in controlled environments, we demonstrate that phosphate starvation response occurs before abscisic acid response in responding to mild drought stress. Our observations in the field and laboratory using model crop and experimental plants provide insight into the molecular response to mild drought in field-grown plants and the relationship between nutrition and drought stress response.

Introduction

Since the beginning of the history of agriculture, droughts have threatened crop production around the world. Drought is a complex and unpredictable natural disaster, with varying patterns of intensity, timing, persistence, and frequency[1]. Numerous studies, mainly in *Arabidopsis thaliana* plants, have revealed that the phytohormone abscisic acid (ABA) plays a crucial role in regulating the responses to a wide variety of drought stress conditions and in optimizing water use in plants. Cellular dehydration increases endogenous ABA levels, which triggers multiple physiological and molecular responses, including stomatal closure and the activation of dehydration/ABA-responsive gene expression[2, 3]. While studies of severe drought stress responses in plants have revealed the underlying molecular mechanisms, such as the ABA signaling pathway, it has recently become clear that different molecular mechanisms are involved in mild or moderate drought stress responses[4-6]. Indeed, not only ABA-related genes but also genes related to photosynthesis, carbohydrate turnover, cell wall expansion, and growth regulation are involved in the response of plants to mild or moderate drought stress conditions[7-11]. However, the molecular mechanisms underlying mild drought stress responses of plants in the field, where the environment fluctuates, remain elusive.

Phosphorus is one of the three major nutrients, along with nitrogen and potassium, that condition plant growth in natural soils. Although phosphorus is abundant in many natural soils as organic and inorganic matter, plant roots absorb only inorganic orthophosphate (Pi), which is also essential for microbial growth[12, 13] and is rarely present in the soil[14]. Plants have therefore evolved a phosphate starvation response (PSR) system that senses phosphate starvation and regulates root and stem growth accordingly[15]. The genetic basis of the PSR has been intensively studied in the model experimental plant *Arabidopsis*[16]. PSR is controlled by a conserved pathway centered on the SPX receptors and PHR transcription factors[17-19]. PHR transcription factors regulate the expression of PSR genes (e.g., those encoding phosphate transporters, phosphatases, and lipid modification proteins) to enhance Pi uptake under Pi-deficit conditions[20]. The establishment of beneficial relationships with some soil microorganisms is one of the strategies for increasing Pi uptake capacity in plants, and genetic mechanisms of the relationship between the PSR and the immune system are emerging[21, 22]. Although it has been reported that drought reduces the amount of Pi in plants[23], the link between the PSR and drought is not well understood.

As a major oil and protein source for food, feed, biodiesel, and industrial products, soybean (*Glycine max* L. Merr.) is the most economically important dicot crop in the world[24] . The growing demand for soybean oil, especially in emerging economies, has led to a rapid increase in soybean production; in recent years, the global production and harvested area of

106 soybean have increased at rates that exceed those of the other major crops[25]. However, since
107 soybean is cultivated mostly under rainfed conditions, soybean production is severely
108 constrained by abiotic stresses, particularly drought[26]. Even mild drought stress that occurs
109 without obvious outward signs of a stress response, such as leaf wilting, poses a major threat
110 to soybean productivity[27]. With this growing importance of soybean and the need for soybean
111 research, techniques have been developed to grow soybean vigorously enough to cross and
112 promote generation in indoor growth chambers with fluorescent lighting, which are commonly
113 used to grow *Arabidopsis* plants[28], and various molecular tools and genomic and mutant
114 resources have accumulated[29]. Thus, soybean is an ideal model crop for bridging the gap
115 between laboratory and field drought stress response mechanism studies, not only because of
116 its economic importance but also because of its well-developed research tools.

117 A wide range of studies have been conducted in controlled environments, such as
118 indoor growth chambers and greenhouses, and in actual fields, to understand the complex and
119 elusive mechanism of the drought stress response in plants in the field[30]. For example, in indoor
120 growth chambers, drought stress tests have been carried out in which plants are removed from
121 agar medium and placed in petri dishes or watering is stopped for plants grown in pots, causing
122 rapid drought stress, and then re-watered, before their survival rates are measured[31]. In
123 greenhouses, drought stress tests have been performed to vary irrigation conditions for plants
124 grown in pots, whereas in the field, the tests have been done in experimental plots with different
125 irrigation conditions and rainout shelters to keep rain out of the test plots[32]. While it is relatively
126 easy to control the growing environment indoors, it is not easy to mimic the complex drought
127 conditions that occur in the field. Field tests do not have the various constraints that are present
128 in pot tests, but the complex changes in the natural environment make it extremely challenging
129 to control environmental conditions such as drought. Although there have been attempts to
130 translate research results from the laboratory to the field, many hurdles remain[33].

131 Here, using soybean as a model field-grown crop during 6 years of trials, we show
132 that ridges are a useful experimental tool for mimicking mild drought stress in the field. Using
133 this method, we determined that mild drought reduces leaf inorganic phosphate levels and
134 activates the PSR in field-grown soybean plants. Detailed pot-based experiments with field soil
135 indicated that PSR-related gene expression is mainly observed under drought conditions that
136 are too mild to activate ABA-mediated gene expression. Furthermore, using *Arabidopsis*, in
137 addition to soybean, we demonstrate that the PSR is initiated before the ABA response during
138 mild drought in plants. Thus, our findings provide insight into the molecular response to mild
139 drought in field-grown plants and the relationship between nutrition and the plant drought
140 stress response. We also show that a field-to-pot approach, in which a phenomenon observed

in the field is examined in pot tests, is an effective strategy for elucidating drought response mechanisms.

Results

Ridges induce mild drought and reduce yields in the field. Understanding how plants respond to drought in the field at the molecular level is quite challenging. For example, the commonly used method of setting irrigated and non-irrigated plots makes it difficult to see the effects of drought on the non-irrigated plots when both plots receive sufficient rainfall[34]. Rainout shelters are an effective way to exclude rainfall from the experimental plots, but fixed shelters with permanently closed roofs have unavoidable effects on microclimate, such as changes in temperature and photosynthetic radiation, and while roofs that close only during rainfall can minimize unintended sheltering effects on microclimate, they are very costly to install and maintain[35]. Perhaps in part because of this situation, most drought experiments have been conducted in areas biased toward Europe and the United States[36] and have not been adapted to local conditions and conducted all over the world. While ridges are widely used in crop production for various purposes, including facilitating drainage, they have not been used to explore the drought stress response in plants at the molecular level. Therefore, we focused on "ridges" to overcome the various problems associated with drought trials in the field and to identify molecular mechanisms in drought response in the field. Soybean, which has the highest water use per kilogram of product among staple crops such as maize, wheat, and rice[37], was used as the model for this field experiment.

For each growing season over six consecutive years, we created flat and ridged plots (referred to as "flats" and "ridges," respectively) in a model experimental field to conduct mild drought tests. We monitored the volumetric water content (VWC) of the soil using soil moisture sensors (Fig. 1a, b; Supplementary Figs. 1-3). In 2016, the soil VWC in the flats of our experimental field fluctuated between 34% (–170 kPa) and 49% (–4 kPa) (Fig. 1c; Supplementary Fig. 4). Although the VWC was strongly affected by rainfall (Fig. 1c), the VWC in ridges (ridge height, 30 cm; Fig. 1a, b) was consistently lower than that of the flats and fluctuated between 27% (–530 kPa) and 41% (–44 kPa) (Fig. 1c; Supplementary Fig. 4). We compared soybean growth on the flats and ridges. The aboveground biomass of the plants grown on ridges was clearly reduced compared with that of plants grown on flats, even though leaf wilting was not observed in either group of plants (Fig. 1d; Supplementary Fig. 5). Thermal imaging analysis of the soybean plants showed that the leaf temperature of the plants grown on ridges was higher than that of plants grown on flats (Fig. 1e), suggesting that transpiration was lower in the plants grown on ridges, which may have reduced the photosynthetic rate and

biomass. Consequently, the yield of soybean grown on ridges was also reduced compared with that of soybean grown on flats (Fig. 1f, g; Supplementary Fig. 6). A decrease in transpiration and growth is a typical response of plants to water deficit, suggesting that ridges induce mild drought stress in plants in the field.

Irrigation can compensate for the reduced growth caused by ridges. To ascertain whether the reduced growth of the plants on ridges was indeed due to water deficit or rather to changes in the nutrient composition of the soil, we measured the nitrogen (N), phosphorus (P), and potassium (K) contents in the flats and ridges. There was no significant difference in the contents of these nutrients between the flats and ridges, both at the beginning and at the end of the soybean growing season (Fig. 1h). We thus next examined whether watering the ridges would compensate for the negative effect of ridges on plant growth (Fig. 2; Supplementary Fig. 7). Among rainfed plants, there was a noticeable difference in soybean growth on flats and ridges, whereas this difference was reduced or barely detectable among irrigated plants (Fig. 2; Supplementary Fig. 7b-e). Thus, the negative effect of ridges on plant growth was complemented by irrigation, indicating that the reduced growth of the plants on ridges was mainly caused by water deficit. While a water deficit was not adequately induced on ridges in 2017, the results of the remaining 5 years of field trials demonstrated that the reduction in soybean growth on ridges compared with flats was a result of reduced VWC (Fig. 1; Supplementary Figs. 7-9). Together, these observations demonstrate that ridges are a valuable tool for inducing conditions that mimic mild drought stress in the field.

PSR is induced in response to mild drought in plants in the field. To examine how mild drought stress affects the expression of genes in soybean plants in the field, we analyzed the fully expanded second trifoliate leaves of 29-day-old pre-flowering plants in the 2015 field experiment using RNA sequencing (RNA-seq) (Fig. 3a, b; Supplementary Fig. 9). We identified 3,045 differentially expressed genes (DEGs) between the soybean plants grown on flats and those grown on ridges (Supplementary Data 1), which had soil VWCs at sampling time of 41% (–26 kPa) and 34% (–123 kPa), respectively (Supplementary Figs. 4 and 9). We identified 990 and 400 DEGs that were up- and down-regulated ($|\log_2(FC)| \geq 1$, FPKM value > 0, $q < 0.05$), respectively, under mild drought conditions (Fig. 3c; Supplementary Data 2 and 3). Gene Ontology (GO) enrichment analysis (false discovery rate [FDR] < 0.05) revealed that various genes not related to ABA but to nutrition, sugars, vitamins, lignin, and carbohydrates were enriched in the up-regulated DEGs, while no GO terms were significantly enriched among the down-regulated DEGs (Supplementary Data 4). Notably, 16 and 7 of the up-regulated

DEGs were related to "cellular response to phosphate starvation" and "phosphate ion homeostasis", respectively (Supplementary Fig. 10). Furthermore, 11.4% of the up-regulated DEGs were PSR genes, including those encoding signaling factors, phosphatases, transporters, and genes implicated in lipid metabolism in *Arabidopsis*[21] and soybean[38, 39] (Fig. 3d, e; Supplementary Data 5 and 6), indicating that a battery of PSR genes were up-regulated under mild drought conditions. Mild drought stress induced the expression of PSR marker genes in not only the second but also the first and third trifoliate leaves of soybean plants in the field (Fig. 3f).

Pi levels decrease in response to mild drought. To determine whether reduced P levels indeed occur under mild drought conditions in the field, we measured Pi concentration of the first to third trifoliate leaves. Pi concentrations in leaves at each of these positions of soybean plants grown on ridges were significantly lower than those of plants grown on flats (Fig. 3g), indicating that mild drought stress decreases Pi levels in the leaves of field-grown soybean plants. Together with our earlier observations (Fig. 1c, e; Supplementary Figs. 7-9), these results suggest that reduced transpiration and water availability induced by mild drought stress inhibit Pi uptake by plants, leading to Pi deficiency conditions. A previous meta-analysis based on 155 observations of plant nitrogen and phosphorus concentrations in a variety of plant species and soils suggested that drought stress has negative effects on plant nitrogen and phosphorus concentrations, with drought conditions inducing a larger decrease of phosphorus than nitrogen[23]. Thus, these findings support the notion that mild drought stress reduces Pi levels to induce the PSR in plants in the field.

Mild drought causes PSR, and more severe drought induces ABA response. We next explored if the link between mild drought stress and the PSR identified in our field experiments could be reproduced in pot trials (Fig. 4). When the primary soybean leaves were fully expanded 10 days after sowing in pots containing the same soil as that used in the field experiments, we started drought stress treatments with five different levels of VWC, α to ε (increasing water deficit; Fig. 4a). Leaf surface temperatures of 26-day-old soybean plants visualized using infrared thermography paralleled soil VWCs in the pots (Fig. 4a, b), suggesting that the lower the VWC, the greater the reduction in transpiration rate under experimental conditions. We analyzed the gene expression profiles of the fully expanded first trifoliate leaves of 38-day-old seedlings grown in pots. Expression levels of PSR genes were largely inversely associated with VWC levels of α to δ, but not ε treatments (Fig. 4c). Thus, soil water status determines the degree of the PSR under mild drought stress conditions,

supporting the findings of our field experiments. Interestingly, even though the VWC decreased between pots δ and ε, PSR gene expression did not increase; by contrast, the expression of ABA-responsive genes, which are established markers of the response to severe drought stress[2, 40], did increase (Fig. 4c, d). Collectively, these data suggest that PSR occurs in milder drought, followed by an ABA response induced by more severe drought (Fig. 4e).

PSR is initiated before ABA response under mild drought in plants. To determine whether the phenomenon of mild drought causing PSR is independent of plant species and soil type, we conducted experiments to induce mild drought using *Arabidopsis* grown in vermiculite, which is commonly used as artificial soil for experiments, and liquid nutrients. Seven-day-old seedlings grown on agar plates were transplanted into pots filled with vermiculite soaked in water containing liquid nutrients and grown for 6 days. The pots were then divided into two groups. Pots containing the control plants were soaked in water, while pots containing the drought-stressed plants were placed on paper towels to reduce soil moisture (Fig. 5a). To further explore the response of plants to water conditions, this experiment also included a rehydration test. After 6 days of drought stress treatment, plants growing in pots that had been soaked in water and left for 1 day were sampled for the rehydration treatment sample. We measured the VWCs of pots and the aboveground biomass of the seedlings after 1, 3, 6, and 7 days of drought stress treatment (Fig. 5b, c). The VWCs of the pots under drought stress conditions decreased gradually and reached approximately 13% after 7 days of drought treatment; the VWC of pots under control conditions was maintained at around 60% during the experiments. No significant difference in aboveground biomass of the seedlings was observed after 1 and 3 days of drought treatment, but the biomass was significantly suppressed after 6 and 7 days of drought treatment compared to the control condition (Fig. 5c). Nevertheless, no wilting was seen in any of the plants under the drought stress condition, indicating that this treatment induced mild drought stress in *Arabidopsis* plants grown in pots (Fig. 5d).

We tested whether mild drought stress causes the PSR in *Arabidopsis* plants grown in pots. We performed RNA-seq of aboveground parts of *Arabidopsis* seedlings in response to mild drought stress and identified 663, 1,158, 1,346, and 871 DEGs ($|\log_2(FC)| \geq 1$, TPM value > 0, $q < 0.05$) after 1, 3, 6, and 7 days of drought treatment (Supplementary Data 7-10), respectively. We observed that 33, 15, 12, and 15% of the up-regulated DEGs after 1, 3, 6, and 7 days of drought treatment were PSR genes, respectively (Fig. 5e; Supplementary Data 6-10), while only 4, 4, 5, and 6% of the DEGs were ABA-inducible genes[40], respectively (Fig. 5e; Supplementary Data 7-11). Hierarchical clustering of 2,397 genes that were differentially expressed ($|\log_2(FC)| \geq 1$, TPM value > 0, $q < 0.05$) in response to mild drought stress in at

least one sampling in the RNA-seq experiments revealed that two gene sets, designated clusters A and B, of the 19 clusters were enriched in genes involved in biological processes related to the PSR and the ABA response (Fig. 5f; Supplementary Data 12). The genes in cluster A were upregulated after 1 day of drought treatment, while those in cluster B were upregulated after 6 days of drought treatment (Fig. 5f, g). Interestingly, cluster A contained 72% of the total PSR genes in the DEGs (97 genes/135 genes), compared to 26% of the total ABA-responsive genes in the DEGs (15 genes/58 genes). In contrast, cluster B contained 64% of the total ABA-responsive genes in the DEGs (37 genes/58 genes), compared to 24% of the total PSR genes in the DEGs (33 genes/135 genes) (Fig. 5f, g). These data show that mild drought stress induces earlier expression of PSR genes than ABA-responsive genes. Together with the results of mild stress trials in soybean plants grown in pots and fields, these results indicate that the PSR precedes the ABA response in plants grown under mild drought conditions. In addition, gene expression of both cluster A and B genes is inactivated by rehydration treatment (Fig. 5f, g). Considering that the biomass of plants after 7 days of drought treatment and plants re-watered for 1 day after 6 days of drought treatment is almost not significantly different (Fig. 5a-c), the difference in gene expression in this experiment reflects differences in the response to soil moisture conditions.

Discussion

Here, we show that the PSR occurs prior to the ABA response in plants under mild drought stress conditions, revealing a novel link between the PSR and drought stress response in plants grown in the field. Based on previous reports of the transcriptomes under mild drought conditions[10, 41-43], it is possible that the novel findings on which this link is based could have been obtained not under artificial experimental conditions with nutrient-rich soils, but in the field, where available P was not abundant and P acquisition was dependent on the biotic and abiotic environment[44]. We conducted pot tests in the greenhouse using field soil and established that mild drought causes the PSR and that more severe drought causes the ABA response. Moreover, to determine whether such induction of PSR under mild drought is a phenomenon unique to soybean grown in the field, we performed experiments using *Arabidopsis*, vermiculite, and liquid nutrients and found that PSR gene induction occurs earlier than ABA-induced gene induction under mild drought. Thus, through these combined analyses of model crop and experimental plants, in the field and in pots in greenhouses and controlled-environment growth rooms, and with the field and artificial soils, new insights into the mild drought response of plants have been obtained. Our results therefore demonstrate the importance of field-to-lab–oriented research, in which phenomena observed in the field are

316 verified in the lab, to decipher the mechanism underlying the plant's response to mild drought
317 stress in the field. We have also shown that it is crucial to combine laboratory and field studies,
318 using both model crop and experimental plants, to compensate for the shortcomings of either
319 system and use the strengths of both.

320 Notably, in our pot experiments, PSR was gradually induced in a stress-dependent
321 manner under mild drought (α to δ), but the PSR induction was reduced under severe drought
322 (ε), while expression of ABA-responsive genes was increased (Fig. 4). Considering that
323 reduced soil moisture limits the diffusion of P in the soil[45] and that the phosphate content in
324 plants decreases under drought conditions[23], our results suggest that Pi uptake is reduced under
325 mild drought conditions but leaf water content is maintained to some extent and that Pi
326 concentration in the leaves is reduced, leading to PSR induction (Fig. 4: α to δ). Under severe
327 drought conditions, given the circumstantial evidence, our observations would support the
328 notion that PSR induction is suppressed by a relative increase in Pi concentration due to a
329 decrease in leaf water content (Fig. 4: ε). By contrast, ABA cannot respond in situations where
330 some water is maintained in the leaf but responds when the leaf is losing water; as a result, the
331 PSR occurs prior to the ABA response (Fig. 4e). Although further studies are needed on the
332 molecular mechanisms of PSR in response to mild drought in plants and their relationship to
333 the behavior of intracellular Pi in response to external water status, our findings clearly indicate
334 that PSR genes, whose expression is induced earlier than ABA-responsive genes, are
335 potentially promising early indicators of mild drought stress in plants. So far, the optimal
336 moisture supply to plants has been calculated by changes in soil moisture contents, which are
337 a feature of the external environment surrounding plants, and by estimating transpiration
338 through analysis of plant surface temperature. However, because appropriate soil moisture
339 conditions for plants vary with plant condition and growth and soil type[46], and because it is
340 difficult to eliminate the effects of solar radiation and wind speed in the field using
341 thermographic analysis[47], there has been a need for methods to properly determine plant
342 moisture stress conditions in the field. Since in addition to ABA-responsive gene expression,
343 the PSR gene expression could be used as an indicator of how plants perceive external moisture,
344 the use of such gene markers, combined effectively with soil moisture and thermographic data,
345 may enable more accurate detection of mild drought stress in plants and optimization of
346 irrigation before field crop yields are affected by mild drought stress.

347 Our consecutive 6-year field trials also demonstrate that ridges are a useful
348 experimental tool for inducing mild drought stress in the field. While ridges are widely used in
349 crop production for various purposes, they have not been used to study drought stress responses
350 in plants. Our research using ridges provides insight into the link between plant nutritional and

drought stress responses and paves the way for elucidating the molecular mechanism of the drought response in field-grown plants. Since it is easy and inexpensive to create ridges in experimental fields, this method of inducing mild drought stress overcomes a major research barrier to deciphering the response of field-grown crops to various degrees of drought stress and is expected to facilitate efforts around the world, even in countries with emerging economies where it may not be possible to build expensive facilities. The effects of mild drought are difficult to determine visually in the field, but they significantly reduce yield, so proper diagnosis is critical for crop development and water management to maintain yields. Global food security depends on producing crops that can maintain productivity even under mild to moderate soil water deficits[48, 49]. Thus, in this regard, our development of technology to induce mild drought through the use of ridges and our identification of the PSR as a novel marker of mild drought stress constitute an important basis for improving future food security.

Materials and Methods

Field experiment. Soybean (*Glycine max* L. Merr.) 'Williams 82', a sequenced model US cultivar[50], was used in this study in all years other than 2019. Soybean 'Enrei', a sequenced model Japanese cultivar[51], was used only in the 2019 field experiment. Field experiments were conducted at the experimental field of the Japan International Research Center for Agricultural Sciences (JIRCAS, 36°03′14″ N, 140°04′46″ E, 24 m above sea level) located in Tsukuba, Ibaraki, Japan, from 2015 to 2020. No fertilizers were applied to the experimental field. To mimic mild drought stress in the experimental field, ridges were created using a rotary tiller after plowing (Supplementary Fig. 1a). In field trials conducted in the 2015–2018 growing seasons, ridges were produced using a TA6 or TA800N tiller (Kubota, Oosaka, Japan) coupled to an RA3 rotary (Kubota) and were 30 cm high and 38 cm wide at the base. In the 2019 and 2020 growing seasons, since the same size rotary was unavailable, ridges were created using a TA800N tiller (Kubota) coupled to a SKB-E15C rotary (Kubota) and were 30 cm high and 63 cm wide at the base. The thickness of A horizon, a topsoil characterized by organic matter accumulation, is greater than 30 cm in the experimental field, so both flat and ridged plots were composed of this topsoil.

In 2015, the experimental layout consisted of two areas with flat and ridged plots (Supplementary Fig. 2a). In each area, three plots were used for analysis. Soybean seeds were sown at 20-cm intervals on August 3rd, and 30 plants were grown per plot. For 5 days after sowing, water was sprayed every day to prompt seed germination. In 2016, the experiment was laid out in a randomized complete block design, including flat and ridged plots, with four blocks for four replicates (Supplementary Fig. 2b). Soybean seeds were germinated on

vermiculite in a temperature-controlled phytotron at JIRCAS (27 ± 6°C), as described previously[28], on July 7th, and 30 healthy and uniform 6-day-old seedlings were planted per plot at 20-cm intervals on July 13th. In 2017, the experimental layout was divided into two areas, one irrigated and the other rainfed. Each area was composed of randomized blocks, including flat and ridged plots, with four replicates (Supplementary Fig. 3a). In the irrigated area, EVAFLOW irrigation tubes (Mitsubishi Chemical Agri Dream, Tokyo, Japan) were installed to supply water to the entire area of each plot. Soybean seeds were sown at 20-cm intervals on July14th, and 15 plants were grown per plot. To avoid drought stress during seedling establishment, all plots, including non-irrigated plots, were surrounded by irrigation tubes and irrigated four times from the day before sowing to 7 days after sowing. Subsequently, the irrigated area was irrigated 20 times during the period from 18 to 95 days after sowing. Too much irrigation may have increased soil moisture throughout the test area and failed to induce adequate water deficit on ridges (Supplementary Fig. 8a). In 2018, the experimental layout consisted of two areas, one irrigated and the other rainfed (Supplementary Fig. 2c). Each area comprised randomized blocks, with flat and ridged plots, and with four replicates. In the irrigated area, each plot was surrounded by irrigation tubes and irrigated nine times during the period from 15 to 53 days after sowing (Supplementary Fig. 7a). Soybean seeds were sown at 20-cm intervals on July 19th, and 25 plants were grown per plot. In 2019, the experiment was laid out in a randomized complete block design, including flat and ridged plots, with four blocks for four replicates (Supplementary Fig. 3b). Seeds were germinated on vermiculite in a temperature-controlled phytotron (27 ± 6°C) on July 12th, and 20 healthy and uniform 6-day-old seedlings were planted per plot at 20-cm intervals. In 2020, the experimental layout consisted of two areas, one irrigated and the other rainfed (Supplementary Fig. 3c). Each area comprised randomized blocks, with flat and ridged plots, and with four replicates. In the irrigated area, each plot was surrounded by irrigation tubes and irrigated only once, at 28 days after sowing (Supplementary Fig. 8c). Seeds were germinated on vermiculite in a temperature-controlled phytotron (27 ± 6°C) on July 30th, and 25 healthy and uniform seedlings were planted per plot at 20-cm intervals on August 6th.

Mild drought stress tests in soybean in a greenhouse using pots. Mild drought stress tests in soybean using pots were conducted in a greenhouse (20 ± 10°C) at JIRCAS to examine how soil volumetric water content (VWC) affects phosphate starvation response (PSR)–related gene expression in soybean. Soybean seeds were germinated on moistened vermiculite in a temperature-controlled phytotron[28], and 5-day-old seedlings were transferred to 350-ml pots filled with A horizon soil collected from the JIRCAS experimental field. Seedlings were grown

under well-watered conditions (up to a VWC of 43%) for 5 days in a greenhouse. When primary leaves were fully expanded at 10 days after sowing, VWC began to be adjusted to five different levels, α (57%), β (50%), γ (43%), δ (36%), and ε (29%), by measuring the weight of the pot and adding water every Monday, Wednesday, and Friday. The ranges of variation in VWCs during the period from day 7 after sowing to day 38 were 42–57% (α), 35–50% (β), 30–43% (γ), 24–36% (δ), and 20–29% (ε). The fully expanded first trifoliate leaves of 38-day-old seedlings were collected and immediately frozen in liquid nitrogen. Total RNA from leaves was used for gene expression analysis.

Mild drought stress tests in *Arabidopsis thaliana* in a growth chamber using pots. *Arabidopsis thaliana* L. accession Columbia-0 (Col-0, CS60000) was grown on GM agar plates for 6 days after stratification[52] with a 16-h-light/8-h-dark cycle (40 ± 10 μmol photons m^{-2} s^{-1}). Six-day-old seedlings grown on GM agar plates were transplanted into each pot (7.7-cm diameter) filled with equal amounts of vermiculite (grain size: <1.5 mm) (Midorisangyou, Fukuoka, Japan). The pots from which the plants were transplanted were soaked in liquid medium (0.1 mM KH_2PO_4, 0.4 mM $MgSO_4$, 0.23 μM H_3BO_3, 0.035 μM $MnCl_2$, 0.001125 μM $CuSO_4$, 0.005 μM Na_2MoO_4, 0.25 mM $Ca(NO_3)_2$, 0.19 μM Na-Fe-EDTA, 0.25 mM KNO_3) and grown for 7 days in an environmentally controlled growth room at 21°C under a 16-h-light/8-h-dark cycle (70 ± 20 μmol photons m^{-2} s^{-1}). For mild drought tolerance tests, the pots were divided into two groups at 13 days after stratification. Pots of control plants were soaked in water, whereas pots of drought-stressed plants were placed on paper towels to reduce soil moisture (Fig. 5a). For rehydration tests, after 6 days of drought stress treatment, plants grown in pots that had been soaked in water and left for 1 day were sampled for the rehydration treatment sample. To determine the aboveground biomasses, the fresh aboveground weights of the six seedlings were measured at 1, 3, 6, and 7 days after treatments. The collected seedlings were immediately frozen in liquid nitrogen. Total RNA from the leaves was used for RNA-seq analysis.

Meteorological data. Meteorological data, such as amount of rainfall, were obtained from the Weather Data Acquisition System of the Institute for Agro-Environmental Sciences, National Agriculture and Food Research Organization (http://www.naro.affrc.go.jp/org/niaes/aws/). The weather station is located at 36°01′ N, 140°07′ E, approximately 5 km from the JIRCAS experimental field.

Evaluation of growth and yield performance of soybean in the field. To investigate the effect of mild drought stress induced by ridges on soybean growth, the aboveground biomass was measured at three time points per growing season in 2015 and 2016. In 2015, five plants (one or two plants per plot), seven plants (two or three plants per plot), and seven plants (two or three plants per plot) were selected randomly for measuring the aboveground biomass at 21, 30, and 44 days after sowing, respectively. In 2016, 12 plants (three plants per plot) were selected randomly for measurements of aboveground biomass at 20, 36, and 50 days after sowing. Dry weight of the aboveground biomass was measured after oven-drying at 65°C for more than 48 h.

Yield of soybean plants in field trials was evaluated during 2015–2020. In 2015, 11 plants (three to four plants per plot) grown on the flat plots and 12 plants (four plants per plot) grown on the ridged plots were selected randomly and harvested on December 1st. The number of seeds per plant and total air-dried seed weight per plant were measured. In 2016, 20 plants (five plants per plot) for each condition were selected and harvested on November 10th. After oven-drying at 65°C for more than 48 h, the following parameters were measured for each plant: number of seeds, total seed weight, stem weight, and pod sheath weight. Harvest index was calculated as total seed weight / (total seed weight + stem weight + pod sheath weight). In 2017, 24 plants (six plants per plot) were selected randomly for each treatment and harvested on November 15th. After oven-drying at 65°C for more than 48 h, the following parameters were measured for each plant: number of seeds, total seed weight, combined stem and pod sheath weight, and plant height. In 2018, 48 plants (12 plants per plot) were selected randomly for each treatment and harvested on November 14th. After oven-drying at 65°C for more than 48 h, the following parameters were measured for each plant: number of seeds, total seed weight, stem and pod sheath weight, plant height, and total branch length. In 2019, 40 plants (10 plants per plot) were selected randomly for each treatment and harvested on November 13th. Since soybean plants were damaged by a typhoon on September 8th, only the total biomass, including seeds, stem, and pod sheath, was measured as preliminary data. In 2020, 40 plants (10 plants per plot) were selected randomly for each treatment and harvested on November 2nd. After oven-drying at 65°C for more than 48 h, the following parameters were measured for each plant: total seed weight and combined stem and pod sheath weight.

Image acquisition. Images of soybean plants were taken using a CPA-T640A thermal imaging infrared camera (CHINO, Tokyo, Japan) according to the manufacturer's protocol. Aerial images of the experimental field were obtained using a Phantom 4 unmanned aerial vehicle (DJI, Shenzhen, China) according to the manufacturer's protocol.

Measurements of soil water contents. Based on a preliminary investigation of soybean roots in the flat and ridged plots in the experimental field of JIRCAS, soil moisture content was measured at 0–20 cm or 0–30 cm, starting from the top of the ridge or the flat, in this study. In 2015, the volumetric water content (VWC, m^3 m^{-3}) at a depth of 0–20 cm was measured in each experimental plot at intervals of approximately 3 days using a Hydrosense II 20-cm-long time domain reflectometry (TDR) probe (Campbell Scientific Inc., UT, USA). *In situ* calibration was conducted using the gravimetric method according to the manufacturer's protocol. Tentative VWC values were measured using the TDR probe, and soils at the measured sites were collected from a depth of 0–20 cm using polyvinyl chloride pipes (4.3 cm in diameter and 20 cm in length). Soil weights including water were determined. After pre-drying at 60°C for more than 24 h, soil samples were removed from the pipes and oven-dried at 105°C for more than 24 h to calculate the gravimetric water content (g g^{-1}). A total of eight points were measured. Gravimetric water content was then converted into VWC by multiplying it by the bulk density (BD, Mg m^{-3}), assuming that water density is 1.0 Mg m^{-3}. Since andosols generally have a high porosity[53] (about 70% in this study) and can be easily compressed, it was difficult to collect an accurate volume of soil from a depth of 0–20 cm using a single pipe in the field. Therefore, to determine the BD of soils from a depth of 0–20 cm, soil samples were carefully collected from a depth of 10–15 cm using 100-ml soil sampling cores (DIK-1801-11; Daiki Rika Kogyo, Saitama, Japan) at 12 points, and dry weights of the 100-ml soil samples were then determined after oven-drying at 105°C for more than 48 h. The average BD of soils from a depth of 0–20 cm was 0.734 ± 0.017 (mean ± SD) Mg m^{-3}. From the relationships between the tentative VWC values recorded by the TDR probe (estimated value) and those determined *in situ* (true value), a calibration formula was obtained: actual VWC = 0.9718 × tentative VWC + 0.1255.

In 2016–2020, the VWC at a depth of 0–30 cm was automatically recorded in each plot every day at 10:00 a.m. using a CS616 30-cm-long TDR probe (Campbell Scientific, Inc.) connected to a CR1000 data logger (Campbell Scientific, Inc.). Soil temperature at a depth of 12–18 cm was also recorded with a 107 temperature probe (Campbell Scientific, Inc.) to correct for the temperature dependence of the TDR probes, according to the manufacturer's protocol. Estimated VWCs recorded by the TDR probes were similarly calibrated using the gravimetric method according to the manufacturer's protocol. Eight TDR probes were selected for the calibration and inserted into plots with temperature probes in the experimental field. Soil samples were collected from four points of the plot using polyvinyl chloride pipes (4.3 cm in diameter and 30 cm in length) and soil weight was determined. Dry weights of the soil samples

were determined as described above. BD was measured at a depth of 0–10 cm and 10–30 cm to determine the BD at a depth of 0–30 cm because the BD differed at each depth under test conditions in the field. To determine the BD of soils at a depth of 0–30 cm, soil samples were carefully collected from depths of 3–8 cm and 20–25 cm using 100-ml soil sampling cores (DIK-1801-11; Daiki Rika Kogyo) at eight points each. The BD for depths of 0–30 cm was determined to be 0.773 Mg m^{-3} from the combined weighted average of the values obtained for depths of 0–10 cm and 10–30 cm. The output period data for each TDR probe at the sampling times were corrected for temperature, and tentative VWCs were calculated according to the manufacturer's protocol. Using the averages of tentative VWC values obtained using the eight probes and the corresponding actual VWCs determined *in situ* at each sampling point, a calibration formula was generated: actual VWC = 0.9397 × tentative VWC + 0.1638.

Measurements of soil nutrients. Soil samples were taken from each plot at a depth of approximately 0–30 cm using a polyvinyl chloride cylinder or soil sampler (DIK-1601; Daiki Rika Kogyo) on July 7 and November 17, 2016, which corresponded to the start and end of the soybean cultivation period, respectively. Samples were air-dried and passed through a 2-mm sieve, and the fine earth obtained was subjected to soil chemical analysis. The oven-dried weight of the fine earth was measured to obtain moisture correction factors that were used to convert nutrient contents of air-dried soil to a dry weight basis.

Total carbon and total nitrogen contents were determined using the dry combustion method with an elemental analyzer (Sumigraph NC-220F; Sumika Chemical Analysis Service, Osaka, Japan). Exchangeable bases (K^+) extracted in 1 M ammonium acetate (pH 7) were measured essentially as described previously[54], except that inductively coupled plasma atomic emission spectroscopy with a ICPE-9000 spectrometer (Shimadzu Corporation, Kyoto, Japan) was used in this study. Available phosphorus was determined using the Bray-II method[55] with a UV-1800 spectrophotometer (Shimadzu Corporation).

Soil water retention curve. Soil samples were collected from a depth of 10–15 cm using 100-ml soil sampling cores (DIK-1801-11; Daiki Rika Kogyo) at six points in each plot. The soil water retention, a relationship between the VWC (θ) and soil water potential (ψ), of each sample was measured using a pressure plate apparatus at a water potential of between –3.9 and –98 kPa, as described previously[56], and with a dew point potentiometer (WP4, Decagon Devices) at values below –310 kPa, as described previously[57]. VWC values at depths of 0–20 cm and 0–30 cm were calculated using BD values at each depth. Averaged VWCs are shown at matric potential values of –3.9, –9.8, –31, –98, –619, and –1554 kPa (Supplementary Fig.

4). Regression curves at depths of 0–20 cm and 0–30 cm were obtained by fitting a hydraulic model[58]using SWRC Fit[59]:

$$\theta = \theta_s \left[\frac{1}{\ln[e + (\psi/a)^n]}\right]^m$$

where θ_s is the saturated VWC, e is the Napier's constant, and a, n, and m are three different soil parameters. The model showed a good fit ($R^2 = 0.985$, $p < 0.001$ for both curves).

Transcriptome analysis of soybean plants grown in the field. Ten plants (three or four plants per plot) were randomly selected from each treatment group, and the first to third trifoliate leaves were collected individually and immediately frozen in liquid nitrogen in the field on September 1, 2015. The frozen second trifoliate leaves were powdered using a multi-bead shocker (Yasui Kikai, Osaka, Japan), and the other leaves were powdered using a mortar and pestle. For RNA-seq analysis, total RNA was extracted from powdered samples of fully expanded second trifoliate leaves using an RNeasy Plant Mini Kit (Qiagen) following the manufacturer's protocol. Total RNA samples extracted from three independent plants per plot were mixed for one replicate, and three biological replicates were performed for each treatment. The extracted RNA was used to construct paired-end libraries using a TruSeq RNA Library Preparation Kit v2 (Illumina). The libraries were sequenced on an Illumina HiSeq 4000 sequencer with a 100-bp paired-end protocol (Macrogen). Trimmomatic v0.36[60] with the options SLIDINGWINDOW:4:20, MINLEN:40, LEADING:20, and TRAILING:20 was used for trimming low-quality reads and adaptor sequences. Trimmed reads were mapped against the reference sequence of 'Williams 82' (Wm82.a2.v1: https://phytozome.jgi.doe.gov/pz/portal.html) using STAR v2.5.1[61] with the options outSJfilterReads: Unique; outFilterMatchNminOverLread: 0.96; and outFilterScoreMinOverLread: 0.8. The FPKM (fragments per kilobase of exon per million mapped reads) of each gene was calculated using Cufflinks v2.2.1[62]. Differential expression analysis was performed using Cuffdiff embedded in Cufflinks v2.2.1[62]. Genes that showed a q value < 0.05 were defined as differentially expressed genes (DEGs) between samples grown on flat and ridged plots. Gene annotation such as homology to *Arabidopsis* genes and GO was obtained from gene annotation information in Wm82.a2.v1 (Gmax_275_Wm82.a2.v1.annotation_info.txt).

A heatmap of up- and down-regulated DEGs was constructed using the 'heatmap.2' function of the gplots package in R software v3.3.3[63]. Representatives of the different types of phosphate starvation–responsive genes were selected among up-regulated genes based on a previous report[21, 38, 39]. GO enrichment analysis using the clusterProfiler package in R[64] was

performed for the up- and down-regulated DEGs, satisfying the following criteria: $|\log_2(FC)| \geq 1$, FPKM value > 0, $q < 0.05$. A directed acyclic graph (DAG) was constructed using the clusterProfiler package in R. GO terms were regarded as significantly enriched when FDR < 0.05. GO descriptions were obtained using AnnotationHub ("AH13355") in R[65].

Transcriptome analysis of *Arabidopsis* plants grown in pots. Total RNA was extracted from three *Arabidopsis* seedlings per pot using RNAiso Plus (Takara Bio, Japan) according to the manufacturer's instructions. Three biological replicates per treatment were performed for RNA-seq analysis. The extracted RNA was used to construct paired-end libraries using a TruSeq Stranded mRNA Sample Prep Kit (Illumina). The libraries were sequenced on an Illumina NovaSeq6000 sequencer with a 151-bp paired-end protocol (Macrogen). Trimmomatic v0.39[60] with the options SLIDINGWINDOW:4:20 and MINLEN:40 was used for trimming low-quality reads and adaptor sequences. Trimmed reads were mapped against the reference sequence of TAIR10 (https://www.arabidopsis.org/) using STAR v2.5.1[61] with the options outSAMstrandField: intronMotif; and outFilterType: BySJout. The mapped reads and TPM (transcripts per million) of each gene were calculated using featureCounts[66] and TPMCalculator[67], respectively. Differential expression analysis was performed using edgeR package version 3.30.3[68]. The up- and down-regulated DEGs satisfying the following criteria, $|\log_2(FC)| \geq 1$, TPM value > 0, and $q < 0.05$, were defined as DEGs between control samples and dry conditions.

Hierarchical clustering of 2,397 genes that were differentially expressed ($|\log_2(FC)| \geq 1$, TPM value > 0, $q < 0.05$) in response to mild drought stress in at least one sampling in the RNA-seq experiments was constructed using the 'heatmap.2' function of the gplots package in R software v3.3.3[63]. Representatives of the different types of PSR genes were selected among up-regulated genes based on a previous report (Supplementary Data 6)[21]. For the ABA-responsive marker gene set (Supplementary Data 11)[40], 193 genes were collected from the top of the gene list of DEGs whose expression was up-regulated at 24 hours after ABA treatment[40], the same number as for PSR.

RT-qPCR analysis. For RT-qPCR analysis, total RNA was extracted from soybean leaves using an RNeasy Plant Mini Kit (Qiagen) or RNAiso Plus (Takara Bio) according to the manufacturer's protocols. Extracted total RNA was treated with RQ1 RNase-free DNase (Promega). Complementary DNA (cDNA) was synthesized using PrimeScript RT Master Mix (Takara Bio). RT-qPCR using GoTaq qPCR Master Mix (Promega) was performed on a QuantStudio7 Flex (Applied Biosystems). Relative amounts of target mRNAs were calculated

using the relative standard curve method and normalized against *actin* (*Glyma.15G050200*) as a reference gene. Primers used in this study are listed in Supplementary Data 13.

Measurements of inorganic phosphate contents. Inorganic phosphate (Pi) contents in soybean leaves were examined using a molybdate colorimetric assay[69, 70]. Frozen powdered leaf samples used for gene expression analysis were also used to analyze Pi content. A total of 20–45 mg of each sample was mixed with 1%, v/v, acetic acid (20 µl/mg sample weight), vortexed for 15 min, and incubated at 42°C for 1 h in a heat block. Following centrifugation at 18,300 *g* for 5 min at room temperature, the supernatant was used for Pi assay. Reaction solutions containing 140 µl molybdate solution (master mix of 6:1 0.42%, w/v, ammonium molybdate in 1 N H_2SO_4 and 10%, w/v, ascorbic acid in water) and 60 µl supernatant were incubated in a 96-well plate at 42°C for 20 min using a thermal cycler. The absorbance of 100 µl of the reaction solutions at 820 nm was measured using a ARVOX3 plate reader (PerkinElmer, MA, USA). The amount of Pi in the solution was calculated using a calibration curve based on diluted phosphorus standard solution (FUJIFILM Wako, Japan).

Statistical analysis. Statistical tests in this study, except for the hypergeometric enrichment analysis of PSR marker genes (Fig. 3d, Fig. 5e) conducted using the R function "phyper," were performed in GraphPad Prism 9 (GraphPad software). An unpaired, two-tailed *t*-test or a one-way analysis of variance (ANOVA) with Tukey's test was used in most experiments. Data shown in Fig. 2 and Supplemental Fig. 7 did not appear to be homoscedastic. Therefore, Brown-Forsythe and Welch ANOVA tests with a Dunnett's T3 multiple comparisons test were used.

Data availability

RNA-seq data are available from the DNA Data Bank of Japan (www.ddbj.nig.ac.jp/) under accession numbers DRA012279 and DRA014734.

Acknowledgments

We thank S. Shu, M. Toyoshima, K. Ozawa, N. Hisatomi, Y. Saito, J. Baba, Y. Shirai, Y. Nakamura, I. Gejima, H. Ohwada, N. Tayama, K. Kawamura, T. Komatsu, and H. Ishiyama for technical assistance, and T. Taji, K. Nakashima, M. Fujita, T. Ogata, and Oscar Rollano-Penaloza for discussions. This work was supported by Grants-in-Aid for Scientific Research (KAKENHI) from the Japan Society for the Promotion of Science (JSPS) (Grant Nos. JP18K05379 to YN; JP21H02158 to YN, YF; JP16K07412, JP24510312 to YF), the Moonshot

Research and Development Program for Agriculture, Forestry and Fisheries by Cabinet Office, Government of Japan [funding agency: the Bio-oriented Technology Research Advancement Institution (BRAIN]; Grant No. JPJ009237), the Science and Technology Research Partnership for Sustainable Development (SATREPS) of the Japan Science and Technology Agency (JST) and the Japan International Cooperation Agency (JICA) (Grant No. JPMJSA1907), and the Ministry of Agriculture, Forestry and Fisheries (MAFF) of Japan.

References

1. Pennisi, E. The blue revolution, drop by drop, gene by gene. *Science* **320**, 171-173 (2008).
2. Fujita, Y., Fujita, M., Shinozaki, K. & Yamaguchi-Shinozaki, K. ABA-mediated transcriptional regulation in response to osmotic stress in plants. *J Plant Res* **124**, 509-525 (2011).
3. Zhang, H., Zhu, J., Gong, Z. & Zhu, J.K. Abiotic stress responses in plants. *Nat Rev Genet* **23**, 104-119 (2022).
4. Skirycz, A. et al. Survival and growth of Arabidopsis plants given limited water are not equal. *Nat Biotechnol* **29**, 212-214 (2011).
5. Claeys, H., Van Landeghem, S., Dubois, M., Maleux, K. & Inze, D. What Is Stress? Dose-Response Effects in Commonly Used in Vitro Stress Assays. *Plant Physiol* **165**, 519-527 (2014).
6. Verslues, P.E. Time to grow: factors that control plant growth during mild to moderate drought stress. *Plant Cell Environ* **40**, 177-179 (2017).
7. Harb, A., Krishnan, A., Ambavaram, M.M. & Pereira, A. Molecular and physiological analysis of drought stress in Arabidopsis reveals early responses leading to acclimation in plant growth. *Plant Physiol* **154**, 1254-1271 (2010).
8. Des Marais, D.L. et al. Physiological genomics of response to soil drying in diverse Arabidopsis accessions. *Plant Cell* **24**, 893-914 (2012).
9. Ma, X., Sukiran, N.L., Ma, H. & Su, Z. Moderate drought causes dramatic floral transcriptomic reprogramming to ensure successful reproductive development in Arabidopsis. *BMC Plant Biol* **14**, 164 (2014).
10. Clauw, P. et al. Leaf Growth Response to Mild Drought: Natural Variation in Arabidopsis Sheds Light on Trait Architecture. *Plant Cell* **28**, 2417-2434 (2016).
11. Dubois, M., Claeys, H., Van den Broeck, L. & Inze, D. Time of day

699 determines Arabidopsis transcriptome and growth dynamics under mild
700 drought. *Plant Cell Environ* **40**, 180-189 (2017).
701 12. Zhu, Q., Riley, W.J., Tang, J. & Koven, C.D. Multiple soil nutrient
702 competition between plants, microbes, and mineral surfaces: model
703 development, parameterization, and example applications in several tropical
704 forests. *Biogeosciences* **13**, 341-363 (2016).
705 13. Richardson, A.E. & Simpson, R.J. Soil microorganisms mediating
706 phosphorus availability update on microbial phosphorus. *Plant Physiol* **156**,
707 989-996 (2011).
708 14. Raghothama, K.G. Phosphate Acquisition. *Annu Rev Plant Physiol Plant Mol*
709 *Biol* **50**, 665-693 (1999).
710 15. Poirier, Y. & Bucher, M. Phosphate transport and homeostasis in Arabidopsis.
711 *Arabidopsis Book* **1**, e0024 (2002).
712 16. Chiou, T.J. & Lin, S.I. Signaling network in sensing phosphate availability in
713 plants. *Annu Rev Plant Biol* **62**, 185-206 (2011).
714 17. Ried, M.K. et al. Inositol pyrophosphates promote the interaction of SPX
715 domains with the coiled-coil motif of PHR transcription factors to regulate
716 plant phosphate homeostasis. *Nat Commun* **12**, 384 (2021).
717 18. Zhou, J. et al. Mechanism of phosphate sensing and signaling revealed by
718 rice SPX1-PHR2 complex structure. *Nat Commun* **12**, 7040 (2021).
719 19. Guan, Z. et al. Mechanistic insights into the regulation of plant phosphate
720 homeostasis by the rice SPX2 - PHR2 complex. *Nat Commun* **13**, 1581
721 (2022).
722 20. Sun, L., Song, L., Zhang, Y., Zheng, Z. & Liu, D. Arabidopsis PHL2 and
723 PHR1 Act Redundantly as the Key Components of the Central Regulatory
724 System Controlling Transcriptional Responses to Phosphate Starvation. *Plant*
725 *Physiol* **170**, 499-514 (2016).
726 21. Castrillo, G. et al. Root microbiota drive direct integration of phosphate stress
727 and immunity. *Nature* **543**, 513-518 (2017).
728 22. Hiruma, K. et al. Root Endophyte Colletotrichum tofieldiae Confers Plant
729 Fitness Benefits that Are Phosphate Status Dependent. *Cell* **165**, 464-474
730 (2016).
731 23. He, M. & Dijkstra, F.A. Drought effect on plant nitrogen and phosphorus: a
732 meta-analysis. *New Phytol* **204**, 924-931 (2014).
733 24. Graham, P.H. & Vance, C.P. Legumes: importance and constraints to greater

use. *Plant Physiol* **131**, 872-877 (2003).

25. Faostat-Production, F. A. O. "Crops and livestock products." accessed on July 2022.

26. Manavalan, L.P., Guttikonda, S.K., Tran, L.S. & Nguyen, H.T. Physiological and molecular approaches to improve drought resistance in soybean. *Plant Cell Physiol* **50**, 1260-1276 (2009).

27. Gebre, M.G. & Earl, H.J. Soil Water Deficit and Fertilizer Placement Effects on Root Biomass Distribution, Soil Water Extraction, Water Use, Yield, and Yield Components of Soybean [Glycine max (L.) Merr.] Grown in 1-m Rooting Columns. *Front Plant Sci* **12**, 581127 (2021).

28. Nagatoshi, Y. & Fujita, Y. Accelerating Soybean Breeding in a CO2-Supplemented Growth Chamber. *Plant Cell Physiol* **60**, 77-84 (2019).

29. Zhang, M. et al. Progress in soybean functional genomics over the past decade. *Plant Biotechnol J* **20**, 256-282 (2022).

30. Verslues, P.E., Agarwal, M., Katiyar-Agarwal, S., Zhu, J. & Zhu, J.K. Methods and concepts in quantifying resistance to drought, salt and freezing, abiotic stresses that affect plant water status. *Plant J* **45**, 523-539 (2006).

31. Fujita, Y. et al. AREB1 is a transcription activator of novel ABRE-dependent ABA signaling that enhances drought stress tolerance in Arabidopsis. *Plant Cell* **17**, 3470-3488 (2005).

32. Prince, S.J. et al. Root xylem plasticity to improve water use and yield in water-stressed soybean. *J Exp Bot* **68**, 2027-2036 (2017).

33. Nelissen, H., Moloney, M. & Inze, D. Translational research: from pot to plot. *Plant Biotechnol J* **12**, 277-285 (2014).

34. Fuganti-Pagliarini, R. et al. Characterization of Soybean Genetically Modified for Drought Tolerance in Field Conditions. *Front Plant Sci* **8**, 448 (2017).

35. Kundel, D. et al. Design and Manual to Construct Rainout-Shelters for Climate Change Experiments in Agroecosystems. *Frontiers in Environmental Science* **6** (2018).

36. Hoover, D.L., Wilcox, K.R. & Young, K.E. Experimental droughts with rainout shelters: a methodological review. *Ecosphere* **9,** 1-14 (2018).

37. Mekonnen, M.M. & Hoekstra, A.Y. The green, blue and grey water footprint of crops and derived crop products. *Hydrology and Earth System Sciences* **15**, 1577-1600 (2011).

38. Li, C. et al. Identification of soybean purple acid phosphatase genes and their expression responses to phosphorus availability and symbiosis. *Ann Bot* **109**, 275-285 (2012).
39. Yao, Z., Tian, J. & Liao, H. Comparative characterization of GmSPX members reveals that GmSPX3 is involved in phosphate homeostasis in soybean. *Ann Bot* **114**, 477-488 (2014).
40. Song, L. et al. A transcription factor hierarchy defines an environmental stress response network. *Science* **354** (2016).
41. Chen, W. et al. Identification and Comparative Analysis of Differential Gene Expression in Soybean Leaf Tissue under Drought and Flooding Stress Revealed by RNA-Seq. *Front Plant Sci* **7**, 1044 (2016).
42. Song, L. et al. Genome-wide transcriptome analysis of soybean primary root under varying water-deficit conditions. *BMC Genomics* **17**, 57 (2016).
43. Marcolino-Gomes, J. et al. Diurnal oscillations of soybean circadian clock and drought responsive genes. *PLoS One* **9**, e86402 (2014).
44. Pang, J., Ryan, M.H., Lambers, H. & Siddique, K.H. Phosphorus acquisition and utilisation in crop legumes under global change. *Curr Opin Plant Biol* **45**, 248-254 (2018).
45. Suriyagoda, L.D.B., Ryan, M.H., Renton, M. & Lambers, H. Plant Responses to Limited Moisture and Phosphorus Availability: A Meta-Analysis. *Advances in Agronomy* 143-200 (2014).
46. Jones, H.G. Monitoring plant and soil water status: established and novel methods revisited and their relevance to studies of drought tolerance. *J Exp Bot* **58**, 119-130 (2007).
47. Jones, H.G. & Leinonen, I. Thermal imaging for the study of plant water relations. *J Agric Meteorol* **59**, 205-217 (2003).
48. Tardieu, F., Simonneau, T. & Muller, B. The Physiological Basis of Drought Tolerance in Crop Plants: A Scenario-Dependent Probabilistic Approach. *Annu Rev Plant Biol* **69**, 733-759 (2018).
49. Gupta, A., Rico-Medina, A. & Cano-Delgado, A.I. The physiology of plant responses to drought. *Science* **368**, 266-269 (2020).
50. Schmutz, J. et al. Genome sequence of the palaeopolyploid soybean. *Nature* **463**, 178-183 (2010).
51. Shimomura, M. et al. The Glycine max cv. Enrei Genome for Improvement of Japanese Soybean Cultivars. *Int J Genomics* **2015**, 358127 (2015).

52. Nagatoshi, Y., Fujita, M. & Fujita, Y. Casein kinase 2 alpha and beta subunits inversely modulate ABA signal output in Arabidopsis protoplasts. *Planta* **248**, 571-578 (2018).

53. Paul Driessen, J.D., Otto Spaargaren,Freddy Nachtergaele "Andosols" in Lecture Notes on the Major Soils of the World. *World Soil Resources Rep. Vol. 94, Food and Agriculture Organization of the United Nations, 2001*.

54. Van Reeuwijk, L.P. "Procedures for Soil Analysis" (Tech. Paper Vol. 9, International Soil Reference and Information Centre (ISRIC), Wageningen, 2002; https://www.isric.org/sites/default/files/ISRIC_TechPap09.pdf).

55. Bray, R.H. & Kurtz, L.T. Determination of total, organic, and available forms of phosphorus in soils. *Soil Science* **59** (1945).

56. Dane, J.H. & Hopmans, J.W. "Pressure plate extractor" in Methods of Soil Analysis, J. H. Dane, G. C. Topp, Eds. (SSSA, Madison, 2002), Part 4: Physical methods, pp. 688–690. (2002).

57. Scanlon, B.R., Andraski, B.J. & Bilskie, J. "Dew point potentiameter" in Methods of soil analysis, Part 4: Physical methods, J. H. Dane, G. C. Topp, Eds. (SSSA, Madison, 2002) pp. 662–665.

58. Fredlund, D.G. & Xing, A. Equations for the soil-water characteristic curve. *Can Geotech J* **31**, 521–532 (1994).

59. Seki, K. SWRC fit – a nonlinear fitting program with a water retention curve for soils having unimodal and bimodal pore structure. *Hydrol Earth Syst Sci Discuss* **4**, 407–437 (2007).

60. Bolger, A.M., Lohse, M. & Usadel, B. Trimmomatic: a flexible trimmer for Illumina sequence data. *Bioinformatics* **30**, 2114-2120 (2014).

61. Dobin, A. et al. STAR: ultrafast universal RNA-seq aligner. *Bioinformatics* **29**, 15-21 (2013).

62. Trapnell, C. et al. Transcript assembly and quantification by RNA-Seq reveals unannotated transcripts and isoform switching during cell differentiation. *Nat Biotechnol* **28**, 511-515 (2010).

63. Warnes, G.R. et al. gplots: Various R programming tools for plotting data, 2016. https://cran.r-project.org/web/packages/gplots/index.html. (2016).

64. Yu, G., Wang, L.G., Han, Y. & He, Q.Y. clusterProfiler: an R package for comparing biological themes among gene clusters. *OMICS* **16**, 284-287 (2012).

65. Morgan, M., Carlson, M., Tenenbaum, D. & Arora, S. AnnotationHub: Client

to access AnnotationHub resources. R package version 2.10.1., 2017. (2017).

66. Liao, Y., Smyth, G.K. & Shi, W. featureCounts: an efficient general purpose program for assigning sequence reads to genomic features. *Bioinformatics* **30**, 923-930 (2014).

67. Vera Alvarez, R., Pongor, L.S., Marino-Ramirez, L. & Landsman, D. TPMCalculator: one-step software to quantify mRNA abundance of genomic features. *Bioinformatics* **35**, 1960-1962 (2019).

68. Robinson, M.D., McCarthy, D.J. & Smyth, G.K. edgeR: a Bioconductor package for differential expression analysis of digital gene expression data. *Bioinformatics* **26**, 139-140 (2010).

69. Ames, B.N. Assay of inorganic phosphate, total phosphate and phosphatases. *Methods in Enzymology* **8,** 115-118 (1966).

70. Chiou, T.J. et al. Regulation of phosphate homeostasis by MicroRNA in Arabidopsis. *Plant Cell* **18**, 412-421 (2006).

Figure legends

Fig. 1. Ridges artificially induce mild drought and reduce soybean yield. a Photograph of the experimental field, including the VWC data collection station, watering tubes, and probes (yellow arrows). **b** Twelve-day-old soybean plants on flat and ridged plots (referred to as "flats" and "ridges," respectively). **c** Daily rainfall (dark green bars) and time course of soil VWC (n = 4) in the flats (blue lines and points) and ridges (pink lines and points) over the study period in the 2016 field. **d** Aboveground biomass (dry weight, DW) per plant grown on flats and ridges (n = 12). F and R denote flats and ridges, respectively. **e** Thermogram and the corresponding digital image of 9-week-old soybean plants grown on flats and ridges in 2016. **f** Total seed weight per plant grown on flats and ridges (n = 20). **g** Seeds from individual representative plants grown on flats and ridges. Bars, 10 cm. **h** Nutrient contents (N, P, and K) of soil in flats and ridges before (July) and after (November) soybean cultivation in 2016 (n = 4). $^{**}P < 0.01$, $^{***}P < 0.001$, Student's t-test; ns, no significant difference. Error bars in C, D, F, and H denote SD.

Fig. 2. Irrigation compensates for the reduced growth of plants on ridges. a Aerial view of 7-week-old soybean plants in the 2018 field. F and R denote flats and ridges, respectively. Left half, irrigated area. Right half, rainfed area. **b** Representative soybean plants from flats and ridges with and without irrigation. Bar, 10 cm. **c** Biological yield (total dry weight of seed,

stem, and pod sheaths) per plant grown on flats and ridges (n = 48). $^{***}P < 0.001$, Brown-Forsythe and Welch ANOVA tests with Dunnett's T3 multiple comparisons test; ns, no significant difference. Error bars denote SD.

Fig. 3. Mild drought induces PSR in field-grown soybean plants. a Positions of the second trifoliate leaves (dotted enclosure) used for RNA-seq analysis in 29-day-old soybean plants grown on flats and ridges in 2015. Bars, 10 cm. **b** Schematic representation of a soybean plant. **c** Heat map of $\log_2$ fold change in expression of 990 up-regulated and 400 down-regulated genes ($|\log_2(FC)| \geq 1$, FPKM value > 0, $q < 0.05$) under mild drought conditions induced by ridges. PSR genes are indicated on the lower row. **d** Ratio of PSR marker genes to the total number of genes, the number of up-regulated genes, and the number of down-regulated genes. **e** Representative up-regulated PSR marker genes under mild drought conditions. **f** PSR gene expression determined using quantitative RT-PCR in the first to third trifoliate leaves of 29-day-old plants grown on ridges and flats in 2015 (n = 9 for the second trifoliate leaves; n = 10 for the first and third trifoliate leaves). F and R denote flats and ridges, respectively. **g** Pi contents of first to third trifoliate leaves of soybean plants grown on ridges and flats; same samples described in (**f**). $^{*}P < 0.05$, $^{**}P < 0.01$, and $^{***}P < 0.001$, one-way analysis of variance (ANOVA) with Tukey's test in ridged versus flat plots for each leaf position; ns, no significant difference. Error bars denote SD.

Fig. 4. Mild drought causes PSR and severe drought induces ABA response in pot-grown soybean plants. a Time-course analysis of VWCs in potted soybean plants with five different moisture contents (n = 6). The range of variation in VWCs during the period from day 7 after sowing (when plants were transplanted into pots) to day 38 (when sampling was performed) is shown on the right. Drought stress treatments were imposed from 10 days after sowing. **b** Thermogram and corresponding digital image of 26-day-old soybean plants in pots. **c-d** Relative expression of PSR (**c**) and ABA-responsive (**d**) genes in the first trifoliate leaves of the 38-day-old plants shown in (**b**), as determined by quantitative RT-PCR (n = 6). $^{*}P < 0.05$, $^{**}P < 0.01$, and $^{***}P < 0.001$, one-way analysis of variance (ANOVA) with Tukey's test in β–ε versus α. Error bars denote SD. **e** Proposed model of the plant's response to increasing levels of water deficit stress in terms of gene expression.

Fig. 5. Mild drought induces earlier expression of PSR genes than ABA-responsive genes in *Arabidopsis* plants. a Schematic overview of the experimental design for control, drought, and rehydration in *Arabidopsis* plants. Pots with 13-day-old plants grown in pots soaked in

909 water with liquid nutrients after transplanting from agar plates were placed on paper towels for
910 drought treatment, soaked in water for control, or placed on paper towels for 6 days and then
911 soaked in water for 1 day for rehydration treatment. The plants were sampled at 1, 3, 6, and 7
912 days after treatment (dat). **b** VWCs at treatment initiation and sampling in potted Arabidopsis
913 plants ($n = 3$). Error bars denote SD. **c** Total aboveground biomass (fresh weight, FW) per pot;
914 six plants were grown per a pot in control and drought conditions ($n = 3$). Error bars denote
915 SD. C, D, and R denote control, drought, and rehydration treatment, respectively. **d**
916 Photographs of *Arabidopsis* seedlings at 1 and 7 days after treatment in control and drought-
917 treated pots. **e** Percentage of PSR or ABA marker genes relative to the total number of genes
918 (white bars), the number of up-regulated genes (red bars), and the number of down-regulated
919 genes (green bars) at each sampling time point. **f** Hierarchical clustering of 2,397 genes that
920 were differentially expressed ($|\log_2(FC)| \geq 1$, TPM value > 0, $q < 0.05$) in response to mild
921 drought stress in at least one sampling in the RNA-seq experiments. Right rows indicate PSR
922 and ABA genes. Two gene sets, designated clusters A and B, of the 19 clusters were enriched
923 in genes involved in biological processes related to PSR and ABA responses. **g** Heat maps of
924 $\log_2$ fold change in expression of representative PSR genes in cluster A.

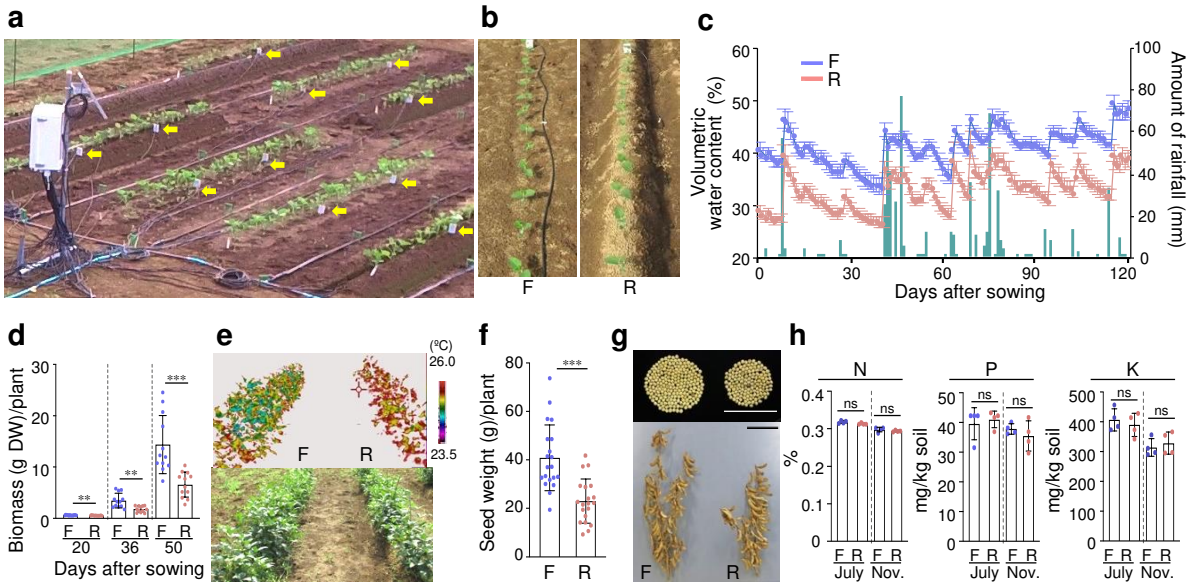

Fig. 1. Ridges artificially induce mild drought and reduce soybean yield. a Photograph of the experimental field, including the VWC data collection station, watering tubes, and probes (yellow arrows). **b** Twelve-day-old soybean plants on flat and ridged plots (referred to as "flats" and "ridges," respectively). **c** Daily rainfall (dark green bars) and time course of soil VWC (n = 4) in the flats (blue lines and points) and ridges (pink lines and points) over the study period in the 2016 field. **d** Aboveground biomass (dry weight, DW) per plant grown on flats and ridges (n = 12). F and R denote flats and ridges, respectively. **e** Thermogram and the corresponding digital image of 9-week-old soybean plants grown on flats and ridges in 2016. **f** Total seed weight per plant grown on flats and ridges (n = 20). **g** Seeds from individual representative plants grown on flats and ridges. Bars, 10 cm. **h** Nutrient contents (N, P, and K) of soil in flats and ridges before (July) and after (November) soybean cultivation in 2016 (n = 4). $^{**}P < 0.01$, $^{***}P < 0.001$, Student's t-test; ns, no significant difference. Error bars in C, D, F, and H denote SD.

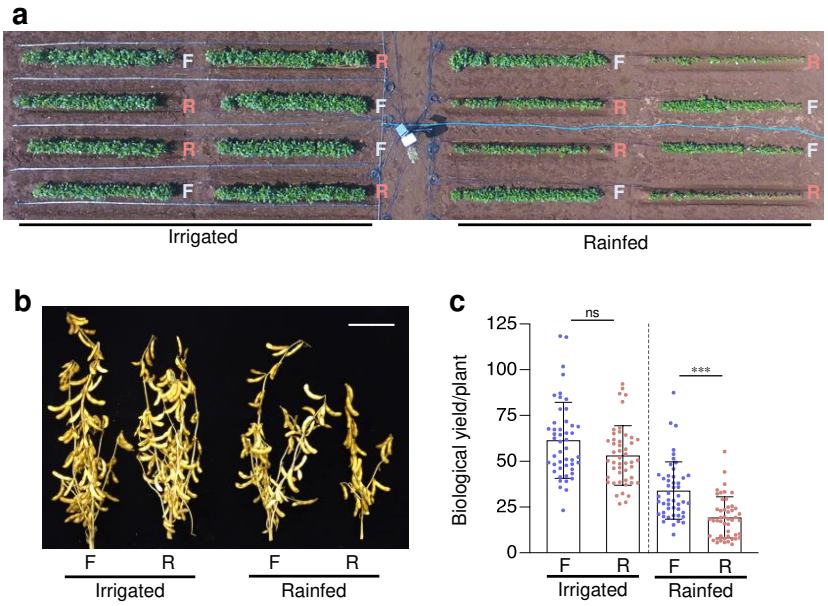

Fig. 2. Irrigation compensates for the reduced growth of plants on ridges. a Aerial view of 7-week-old soybean plants in the 2018 field. F and R denote flats and ridges, respectively. Left half, irrigated area. Right half, rainfed area. **b** Representative soybean plants from flats and ridges with and without irrigation. Bar, 10 cm. **c** Biological yield (total dry weight of seed, stem, and pod sheaths) per plant grown on flats and ridges (n = 48). $^{***}P < 0.001$, Brown-Forsythe and Welch ANOVA tests with Dunnett's T3 multiple comparisons test; ns, no significant difference. Error bars denote SD.

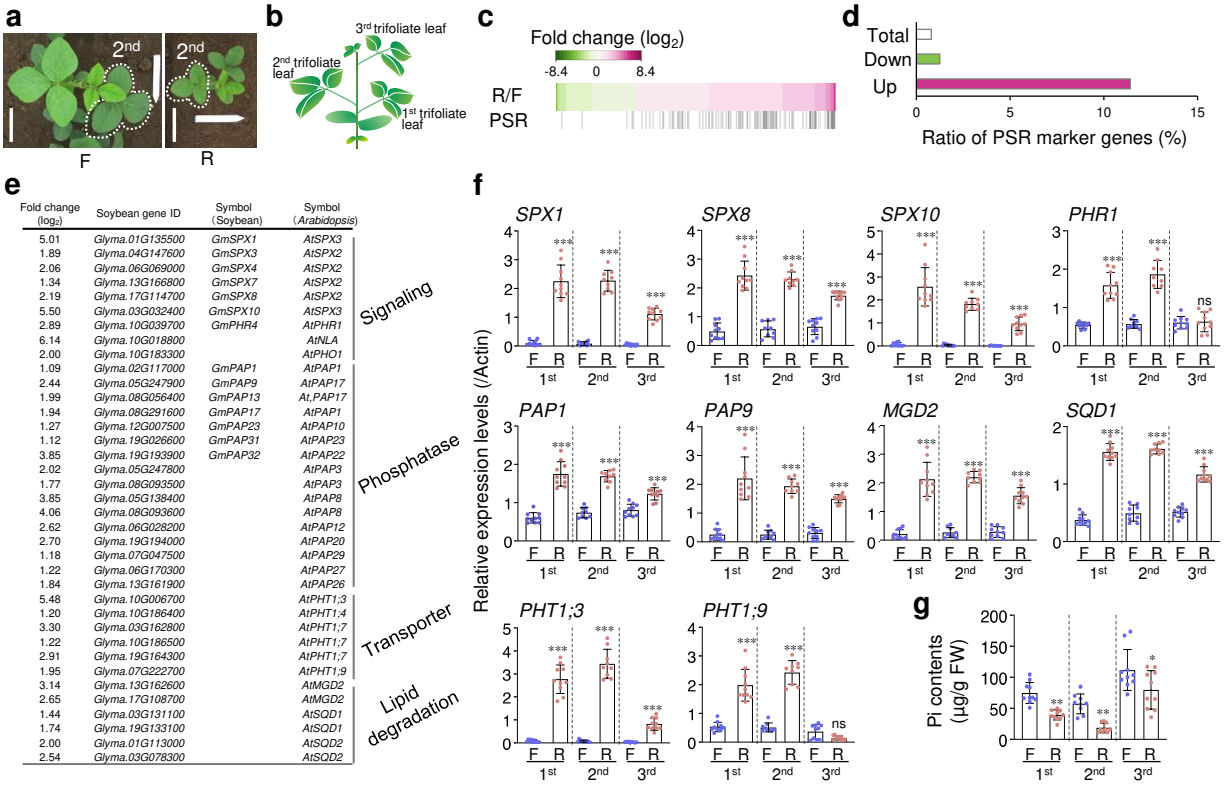

Fig. 3. Mild drought induces PSR in field-grown soybean plants. a Positions of the second trifoliate leaves (dotted enclosure) used for RNA-seq analysis in 29-day-old soybean plants grown on flats and ridges in 2015. Bars, 10 cm. **b** Schematic representation of a soybean plant. **c** Heat map of $\log_2$ fold change in expression of 990 up-regulated and 400 down-regulated genes ($|\log_2(FC)| \geq 1$, FPKM value > 0, $q < 0.05$) under mild drought conditions induced by ridges. PSR genes are indicated on the lower row. **d** Ratio of PSR marker genes to the total number of genes, the number of up-regulated genes, and the number of down-regulated genes. **e** Representative up-regulated PSR marker genes under mild drought conditions. **f** PSR gene expression determined using quantitative RT-PCR in the first to third trifoliate leaves of 29-day-old plants grown on ridges and flats in 2015 ($n = 9$ for the second trifoliate leaves; $n = 10$ for the first and third trifoliate leaves). F and R denote flats and ridges, respectively. **g** Pi contents of first to third trifoliate leaves of soybean plants grown on ridges and flats; same samples described in (**f**). $^{*}P < 0.05$, $^{**}P < 0.01$, and $^{***}P < 0.001$, one-way analysis of variance (ANOVA) with Tukey's test in ridged versus flat plots for each leaf position; ns, no significant difference. Error bars denote SD.

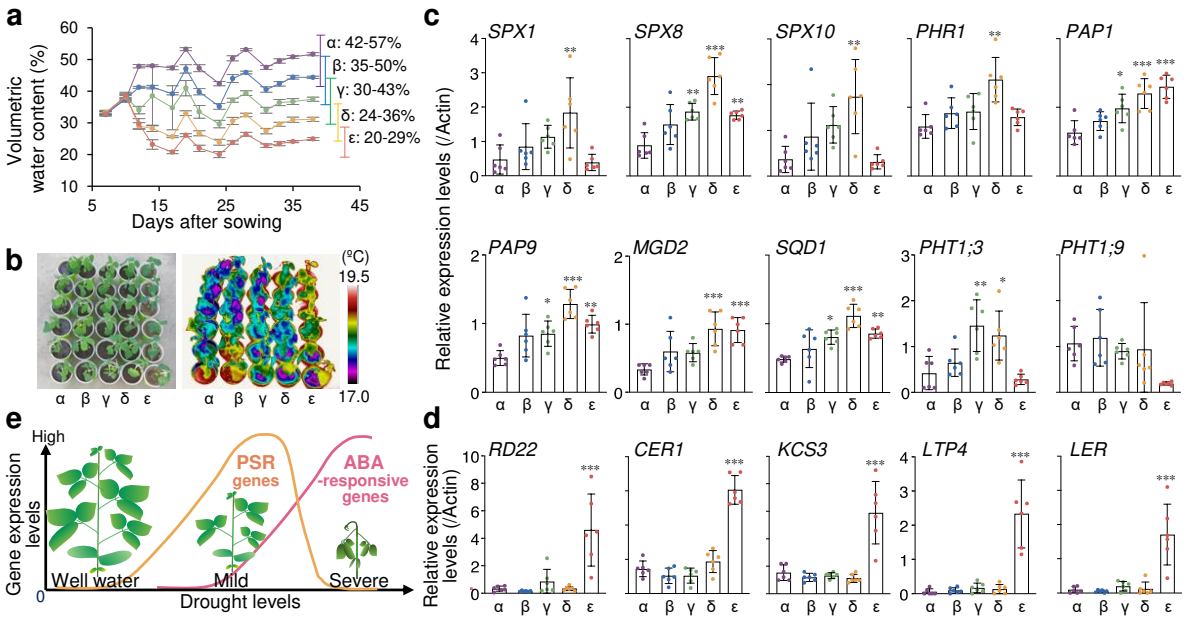

Fig. 4. Mild drought causes PSR and severe drought induces ABA response in pot-grown soybean plants. a Time-course analysis of VWCs in potted soybean plants with five different moisture contents (n = 6). The range of variation in VWCs during the period from day 7 after sowing (when plants were transplanted into pots) to day 38 (when sampling was performed) is shown on the right. Drought stress treatments were imposed from 10 days after sowing. **b** Thermogram and corresponding digital image of 26-day-old soybean plants in pots. **c-d** Relative expression of PSR (**c**) and ABA-responsive (**d**) genes in the first trifoliate leaves of the 38-day-old plants shown in (**b**), as determined by quantitative RT-PCR (n = 6). $^{*}P < 0.05$, $^{**}P < 0.01$, and $^{***}P < 0.001$, one-way analysis of variance (ANOVA) with Tukey's test in β–ε versus α. Error bars denote SD. **e** Proposed model of the plant's response to increasing levels of water deficit stress in terms of gene expression.

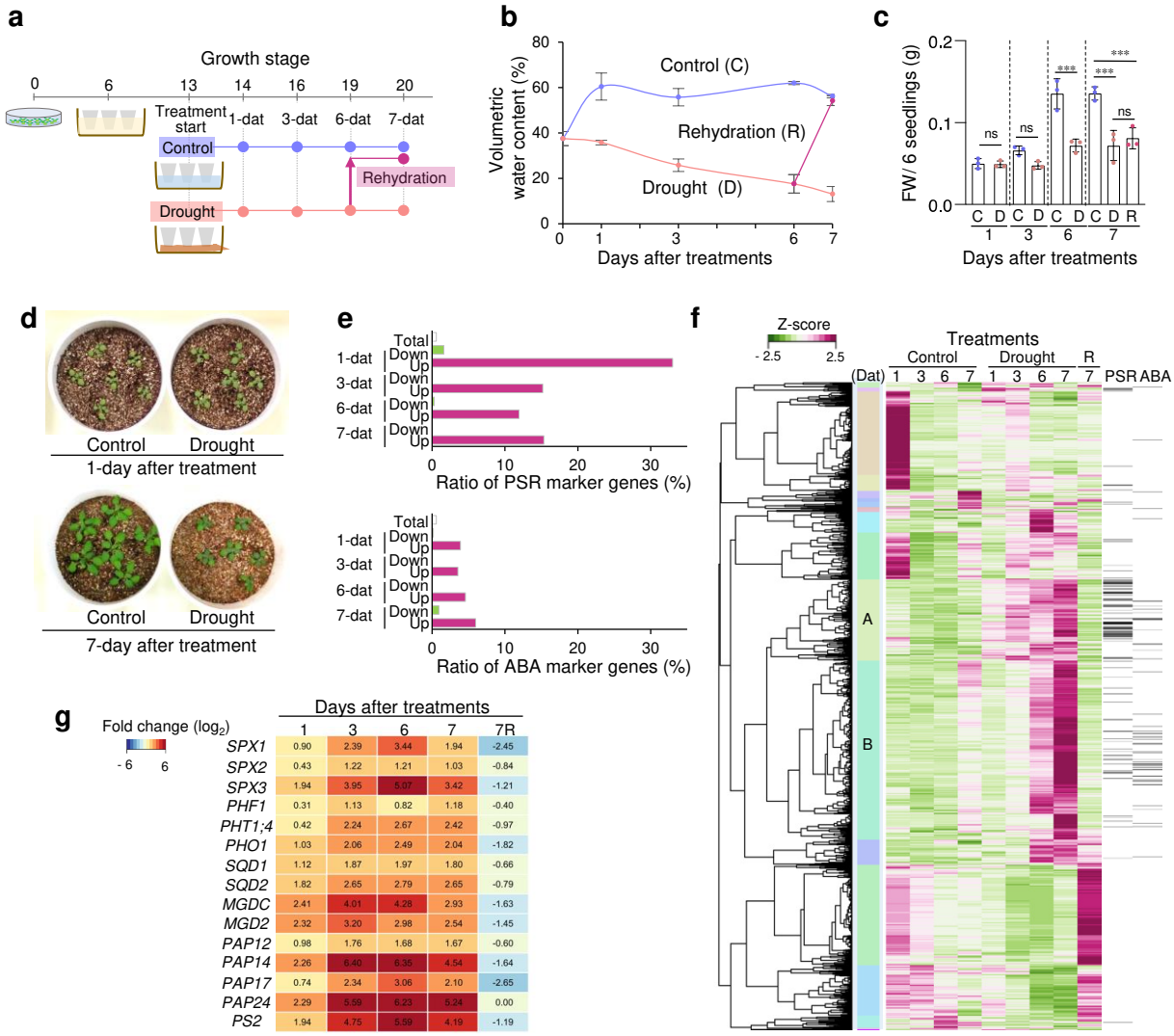

Fig. 5. Mild drought induces earlier expression of PSR genes than ABA-responsive genes in *Arabidopsis* plants. a Schematic overview of the experimental design for control, drought, and rehydration in *Arabidopsis* plants. Pots with 13-day-old plants grown in pots soaked in water with liquid nutrients after transplanting from agar plates were placed on paper towels for drought treatment, soaked in water for control, or placed on paper towels for 6 days and then soaked in water for 1 day for rehydration treatment. The plants were sampled at 1, 3, 6, and 7 days after treatment (dat). **b** VWCs at treatment initiation and sampling in potted Arabidopsis plants (n = 3). Error bars denote SD. **c** Total aboveground biomass (fresh weight, FW) per pot; six plants were grown per a pot in control and drought conditions (n = 3). Error bars denote SD. C, D, and R denote control, drought, and rehydration treatment, respectively. **d** Photographs of *Arabidopsis* seedlings at 1 and 7 days after treatment in control and drought-treated pots. **e** Percentage of PSR or ABA marker genes relative to the total number of genes (white bars), the number of up-regulated genes (red bars), and the number of down-regulated genes (green bars) at each sampling time point. **f** Hierarchical clustering of 2,397 genes that were differentially expressed ($|\log_2(FC)| \geq 1$, TPM value > 0, $q < 0.05$) in response to mild drought stress in at least one sampling in the RNA-seq experiments. Right rows indicate PSR and ABA genes. Two gene sets, designated clusters A and B, of the 19 clusters were enriched in genes involved in biological processes related to PSR and ABA responses. **g** Heat maps of $\log_2$ fold change in expression of representative PSR genes in cluster A.

Supplementary Fig. 1

Supplementary Figure 1. Experimental field plot, equipped with soil moisture sensors and an irrigation system, for analysis of ridge-induced mild drought. a Ridge made using a tiller coupled to a rotary used in this study. **b** Time domain reflectometry (TDR) probes inserted into the soil to measure volumetric water content (VWC) over time during the cultivation period. **c,d** Soil VWC data collected from TDR probes inserted into the soil are sent to a Campbell CR1000 data logger (**c**) through coaxial cables (black cables) in a VWC data collection station (white box) powered by a solar panel (**d**). **e** The VWC data collection station was installed on a tower in the center of the experimental field equipped with an irrigation system. The area on the right was irrigated, whereas that on the left was not.

Supplementary Fig. 2

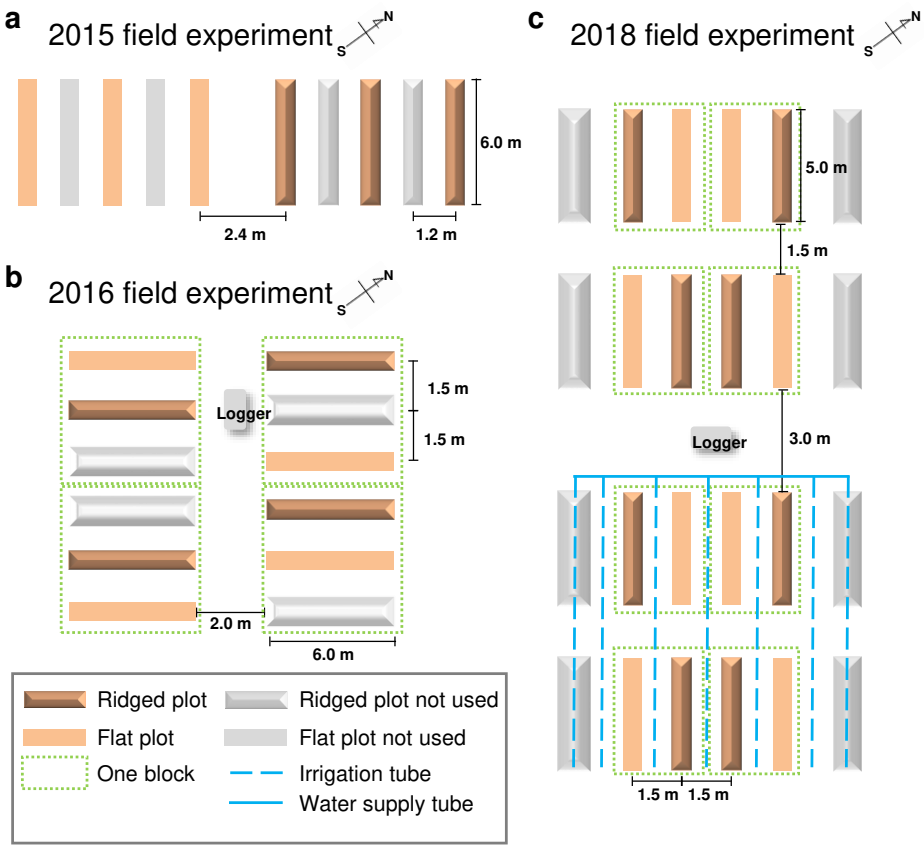

Supplementary Figure 2. Schematic layouts of the experimental plots in 2015, 2016, and 2018. ***a*** In 2015, the experimental layout consisted of two areas, one with flat plots (left) and the other with ridged plots (right). In each area, three plots were used for the analysis. The other two plots in each area were not analyzed in this study. **b** In 2016, the experiment was laid out in a randomized complete block design, including flat and ridged plots, with four blocks for four replicates. Each block included a wider ridged plot that was not analyzed in this study. To monitor soil VWCs over time, TDR probes and a VWC data collection station with a built-in data logger were installed from 2016 onwards (*SI Appendix,* Fig. S1). **c** In 2018, the layout consisted of two separate areas, one irrigated and the other exclusively rainfed. Each area consisted of randomized blocks, each including flat and ridged plots, with four replicates. Wider ridges were constructed along the length of each block, on either side, and were not analyzed in this study.

Supplementary Fig. 3

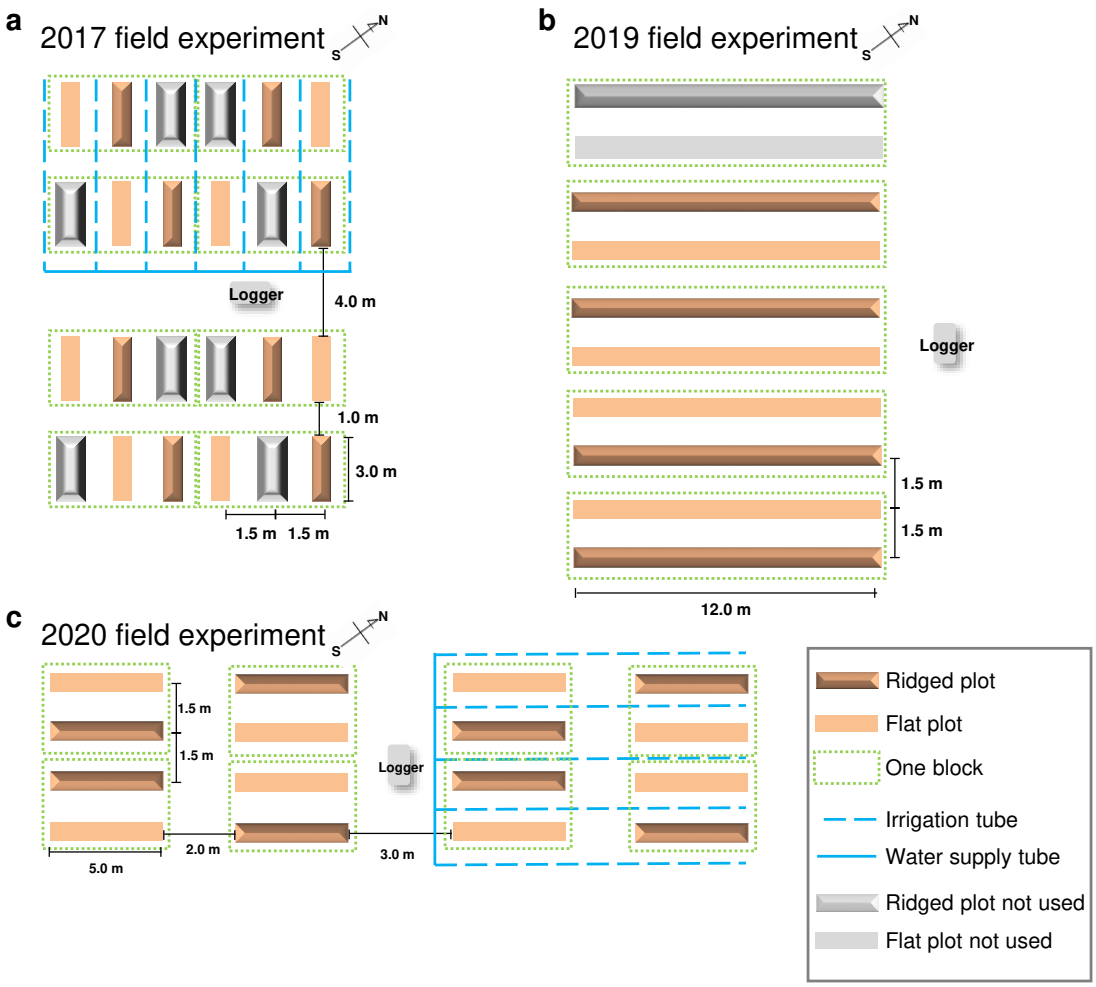

Supplementary Figure 3. Schematic layouts of the experimental plots in 2017, 2019, and 2020. ***a*** In 2017, the experiment layout was divided into two areas, one irrigated and the other exclusively rainfed. Each area included randomized blocks with flat and ridged plots, and with four replicates. Each block included a ridged plot with a wider base, which was not analyzed in this study. **b** In 2019, the experiment was laid out in a randomized block design, including flat and ridged plots, with four blocks for four replicates. The upper side of one block contained flats and ridged plots that were not analyzed in this study. **c** In 2020, the experimental layout was divided into two areas, one irrigated and the other exclusively rainfed. Each area included randomized blocks, including flat and ridged plots, with four replicates.

Supplementary Fig. 4

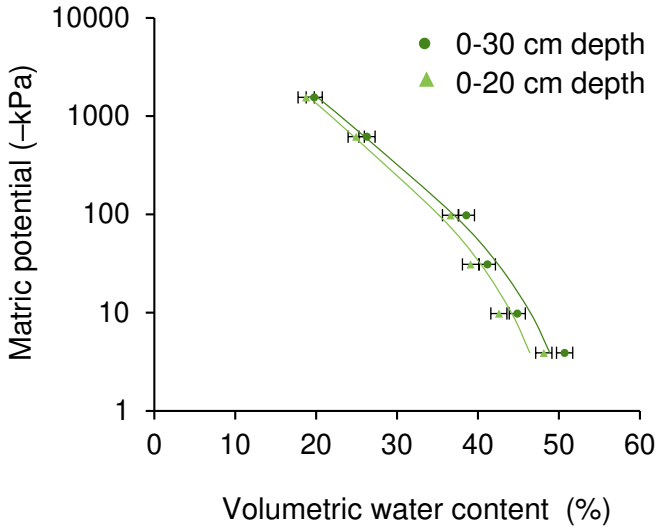

Supplementary Figure 4. Relationship between VWC and matric potential of the soil in the experimental field. Soil samples collected from the experimental field were used to measure the soil water retention. Dark green dots and light green triangles indicate the matric potential at a depth of 0–30 cm (BD value = 0.773) and 0–20 cm (BD value = 0.734), respectively (n = 6). For soil VWCs, VWCs at depths of 0–20 cm, starting from the top of the ridge or the flat, were measured in the 2015 field trials, and VWCs at depths of 0–30 cm, starting from the top of the ridge or the flat, were measured in the 2016 and subsequent field trials. Error bars denote SD.

Supplementary Fig. 5

Supplementary Figure 5. **Growth of soybean plants on the flat and ridged plots at various growth stages in the 2016 field experiment. a** Representative 20-, 36-, and 50-day-old soybean plants grown on flat and ridged plots. Bars, 10 cm. **b** Representative 20-, 36-, and 50-day-old soybean plants in the field, on flat and ridged plots. Differences in soil color reflect the soil moisture at the time of sampling.

Supplementary Fig. 6

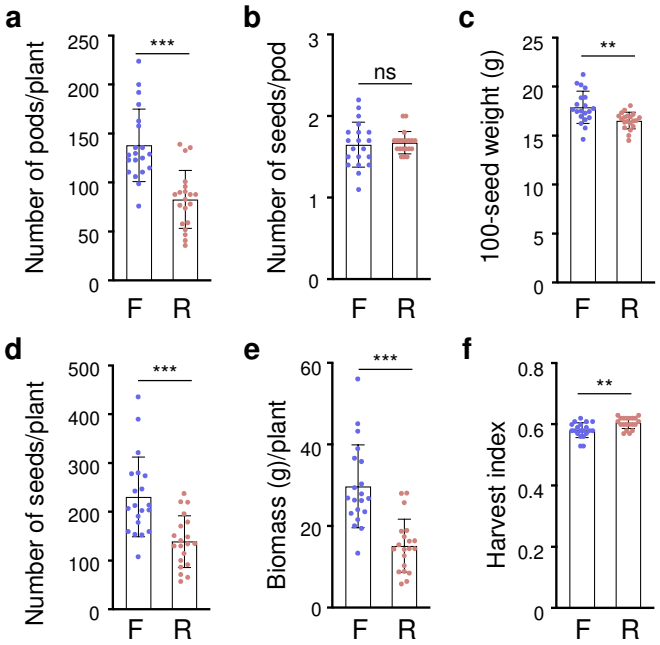

Supplementary Figure 6. Yield components of soybean grown on flat and ridged plots in the 2016 field experiment. a-f Measured values of yield components of soybean grown on flat and ridged plots in the 2016 field experiment. F and R denote flat and ridged plots, respectively. Number of pods per plant (**a**), number of seeds per pod (**b**), 100-seed weight (**c**), number of seeds per plant (**d**), dried aboveground biomass consisting of stem and pods (**e**), and calculated values of harvest index (**f**) of plants grown on the flat and ridged plots (n = 20). $^{**}P < 0.01$, $^{***}P < 0.001$, Student's t-test; ns, no significant difference. Error bars denote SD.

Supplementary Fig. 7

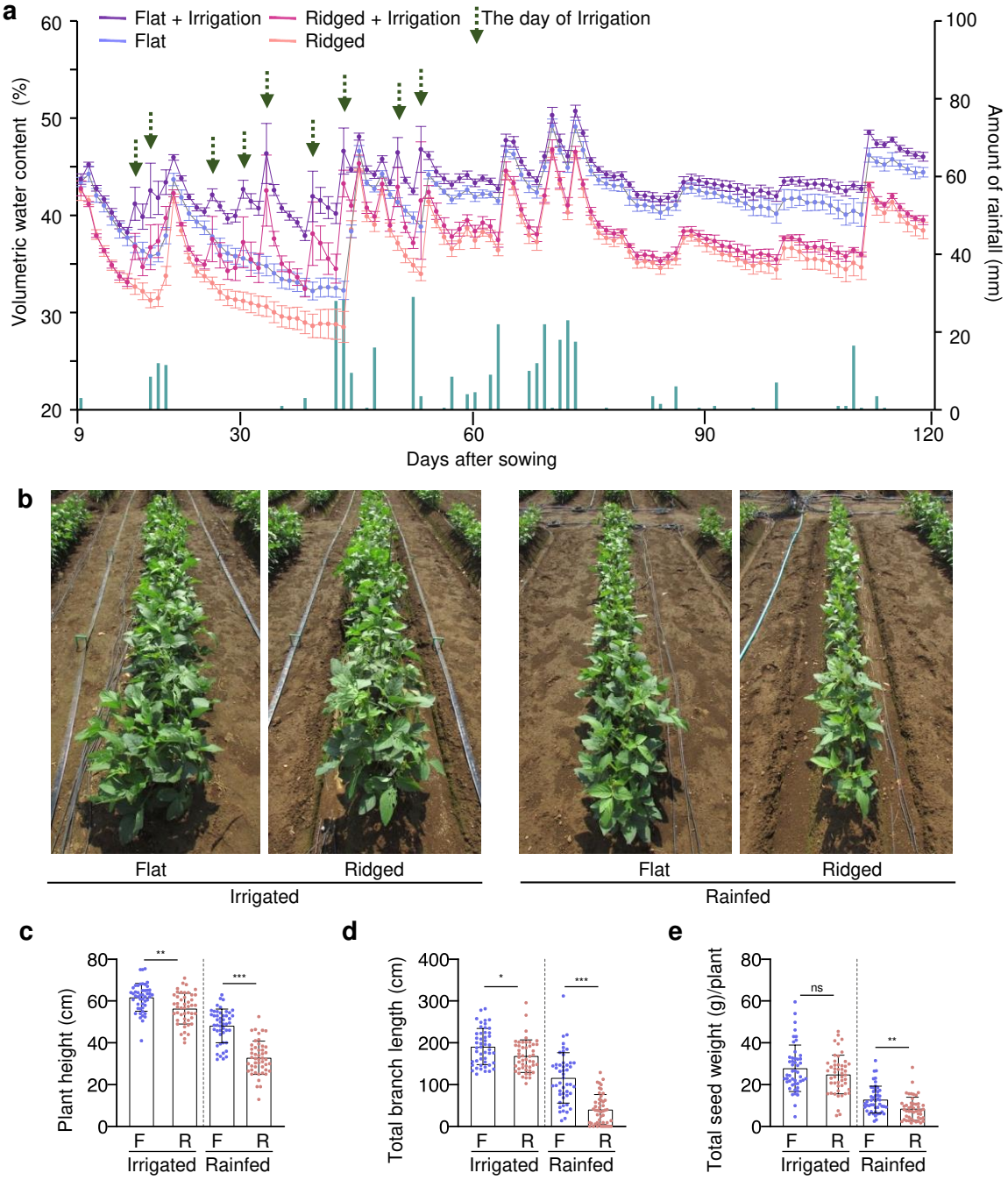

Supplementary Figure 7. Irrigation compensated for the reduced growth of plants on ridges in the 2018 field experiment. a Daily rainfall (dark green bars) and time-course of the soil VWCs (n = 4) in the flat (blue and purple lines and points) and ridged (pink and red lines and points) plots with (purple and red lines and points) and without (blue and pink lines and points) irrigation over the growing period in 2018. Dashed green arrows indicate the day of irrigation. **b** Forty-nine-day-old soybean plants on the flat and ridged plots with and without irrigation. **c-e** Plant height (**c**), total branch length (**d**), and total seed weight per plant (**e**) of the plants grown on the flat and ridged plots with (irrigated) and without (rainfed) irrigation (n = 12). F and R denote flat and ridged plots, respectively. $^{*}P < 0.05$, $^{**}P < 0.01$, $^{***}P < 0.001$ [Brown-Forsythe and Welch ANOVA tests with Dunnett's T3 multiple comparisons test], in R versus the corresponding F value. ns, no significant difference. Error bars in (**a**), (**c**), (**d**), and (**e**) denote SD.

Supplementary Fig. 8

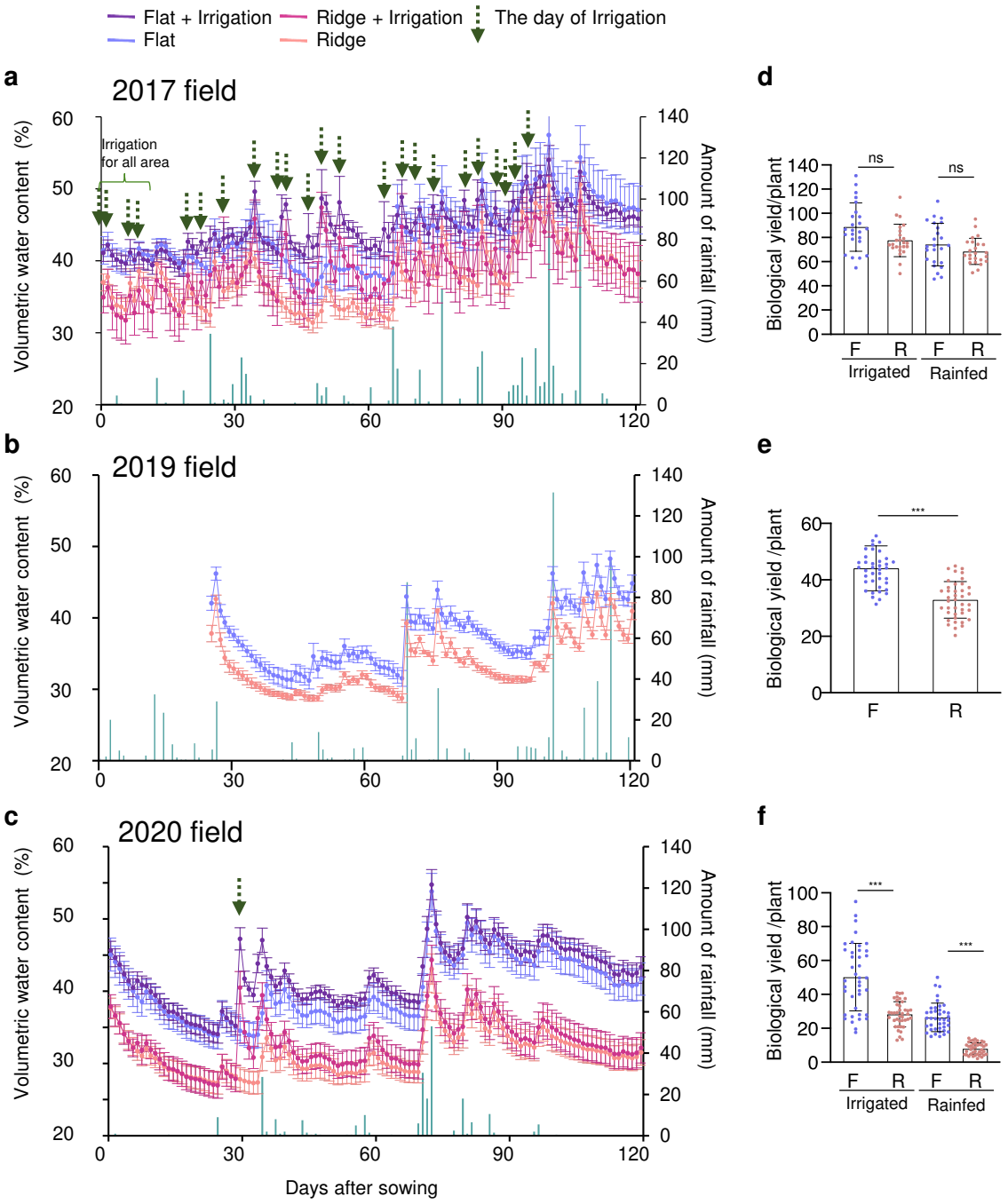

Supplementary Figure 8. Ridges reduce soil water contents in the field. a-c Daily rainfall (dark green bars) and time-course of the soil VWCs (n = 4) in the flat (blue and purple lines and points) and ridged (pink and red lines and points) plots with (purple and red lines and points) and without (blue and pink lines and points) irrigation over the growing period in 2017 (**a**), 2019 (**b**), and 2020 (**c**). Dashed green arrows indicate the day of irrigation. Error bar = SD. **d-f** The biological yield of the harvested soybean grown on flat (blue dots) and ridged (pink dots) plots with (irrigated) or without (rainfed) irrigation. F and R denote flat and ridged plots, respectively. n = 24 (**d**), n = 40 (**e, f**). Error bars denote SD. $^{***}P < 0.001$ and ns indicates not significant in the ridged versus corresponding flat value (Brown-Forsythe and Welch ANOVA tests with Dunnett's T3 multiple comparisons test, **d** and **f**; Student's t-test, **e**). Error bars in (d-f) denote SD.

Supplementary Fig. 9

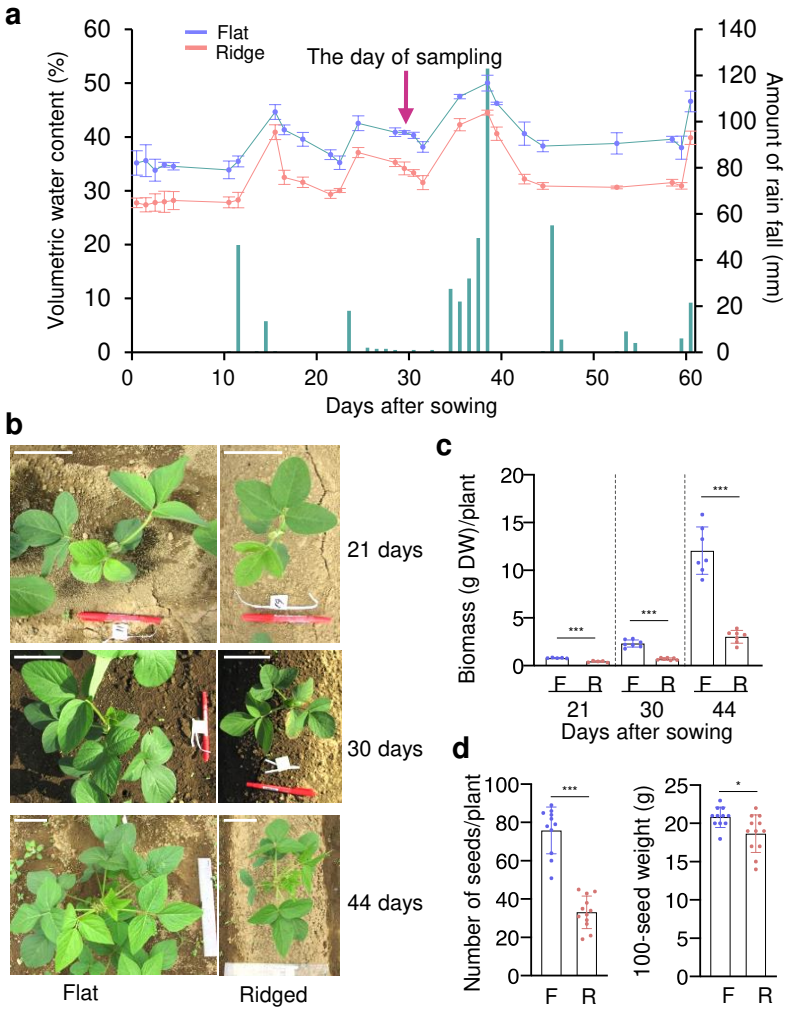

Supplementary Figure 9. **Ridges induced mild drought and hampered soybean growth in the 2015 field experiment. a** Daily rainfall (dark green bars) and time-course of the soil VWCs (n = 3) in the flat (blue lines and dots) and ridged (pink lines and dots) plots over the growing period in the 2015 field. Magenta arrow indicates the day of sampling for RNAseq analysis. **b** Representative 21-, 30-, and 44-day-old soybean plants on the flat and ridged plots. Bars, 10 cm. **c** Aboveground biomass (dry weight) per plant of 21-, 30-, and 44-day-old plants grown on the flat and ridged plots (n = 5 or 7). F and R denote flat and ridged plots, respectively. **d** Number of seeds per plant (left) and 100-seed weight (right) of the harvested plants grown on the flat and ridged plots (n = 10 or 11). $^{*}P < 0.05$, $^{***}P < 0.001$, Student's t-test. Error bars in (**a**), (**c**), and (**d**) denote SD.

Supplementary Fig. 10

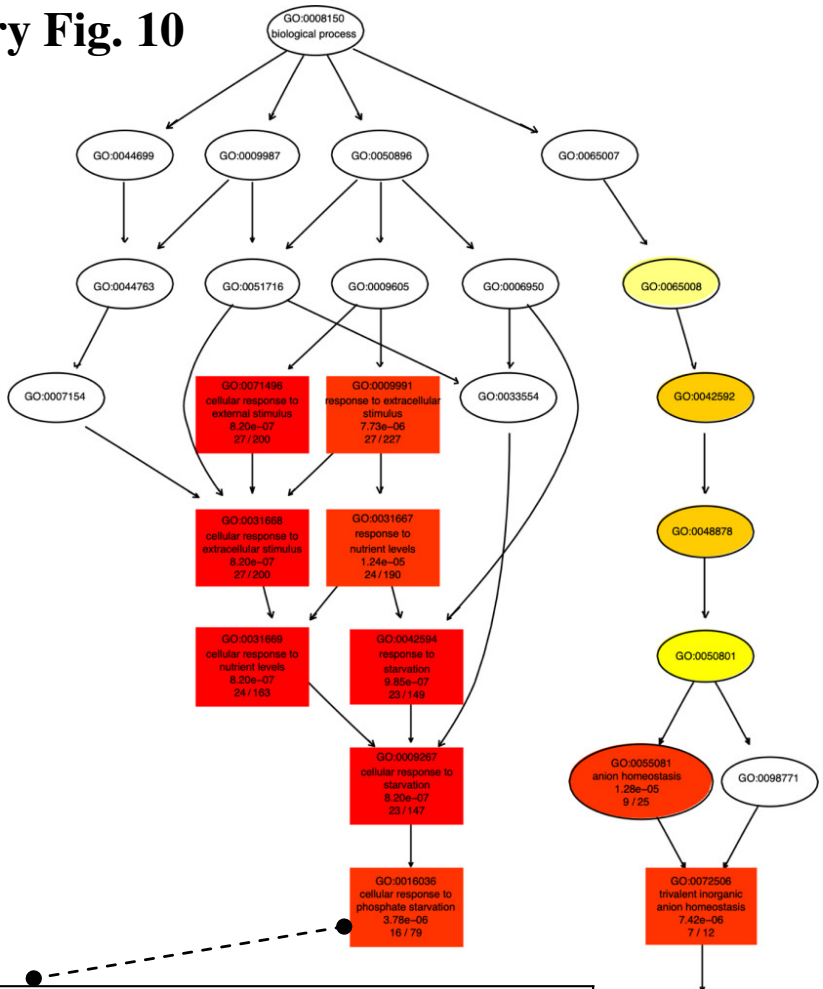

Gene ID	Best BLAST-hit-Arabidopsis gene	
	Gene ID	Annotation
Glyma.10G006700	*AT5G43360.1*	phosphate transporter 1;3
Glyma.08G195000	*AT1G17710.1*	Pyridoxal phosphate phosphatase-related protein
Glyma.07G011900	*AT1G17710.1*	Pyridoxal phosphate phosphatase-related protein
Glyma.03G162800	*AT3G54700.1*	phosphate transporter 1;7
Glyma.06G028200	*AT2G27190.1*	purple acid phosphatase 12
Glyma.13G270400	*AT3G14940.1*	phosphoenolpyruvate carboxylase 3
Glyma.07G222700	*AT1G76430.1*	phosphate transporter 1;9
Glyma.13G351600	*AT1G17710.1*	Pyridoxal phosphate phosphatase-related protein
Glyma.10G166600	*AT1G08650.1*	phosphoenolpyruvate carboxylase kinase 1
Glyma.13G161900	*AT5G34850.1*	purple acid phosphatase 26
Glyma.03G251400	*AT3G04530.1*	phosphoenolpyruvate carboxylase kinase 2
Glyma.20G222600	*AT1G08650.1*	phosphoenolpyruvate carboxylase kinase 1
Glyma.19G200000	*AT3G11670.1*	UDP-Glycosyltransferase superfamily protein
Glyma.12G007500	*AT2G16430.2*	purple acid phosphatase 10
Glyma.10G186500	*AT3G54700.1*	phosphate transporter 1;7
Glyma.10G186400	*AT2G38940.1*	phosphate transporter 1;4

Gene ID	Best BLAST-hit-Arabidopsis gene	
	Gene ID	Annotation
Glyma.05G138400	*AT2G01890.1*	purple acid phosphatase 8
Glyma.06G028200	*AT2G27190.1*	purple acid phosphatase 12
Glyma.16G052000	*AT5G41080.1*	PLC-like phosphodiesterases superfamily protein
Glyma.13G161900	*AT5G34850.1*	purple acid phosphatase 26
Glyma.08G093500	*AT1G14700.1*	purple acid phosphatase 3
Glyma.09G223700	*AT3G47420.1*	phosphate starvation-induced gene 3
Glyma.12G007500	*AT2G16430.2*	purple acid phosphatase 10

Supplementary Figure 10. Mild drought induces the expression of many PSR genes in soybean plants in the field. Gene Ontology (GO) term enrichment analysis of genes up-regulated in soybean under ridge-induced mild drought conditions. GO analysis (FDR < 0.05, p < 0.05) revealed a total of 53 GO terms, mainly involving stress-responsive genes, that were significantly enriched in up-regulated DEGs. Notably, among the up-regulated DEGs, 16 and 7 were related to "cellular response to phosphate starvation" and "phosphate ion homeostasis", respectively. The enriched GO terms are visualized in a directed acyclic graph (DAG) with colors representing the p value (red shows a lower p value than yellow).